Akaroa Harbour Modelling Report

Akaroa Wastewater Project

Prepared for CH2M Beca Ltd

April 2014

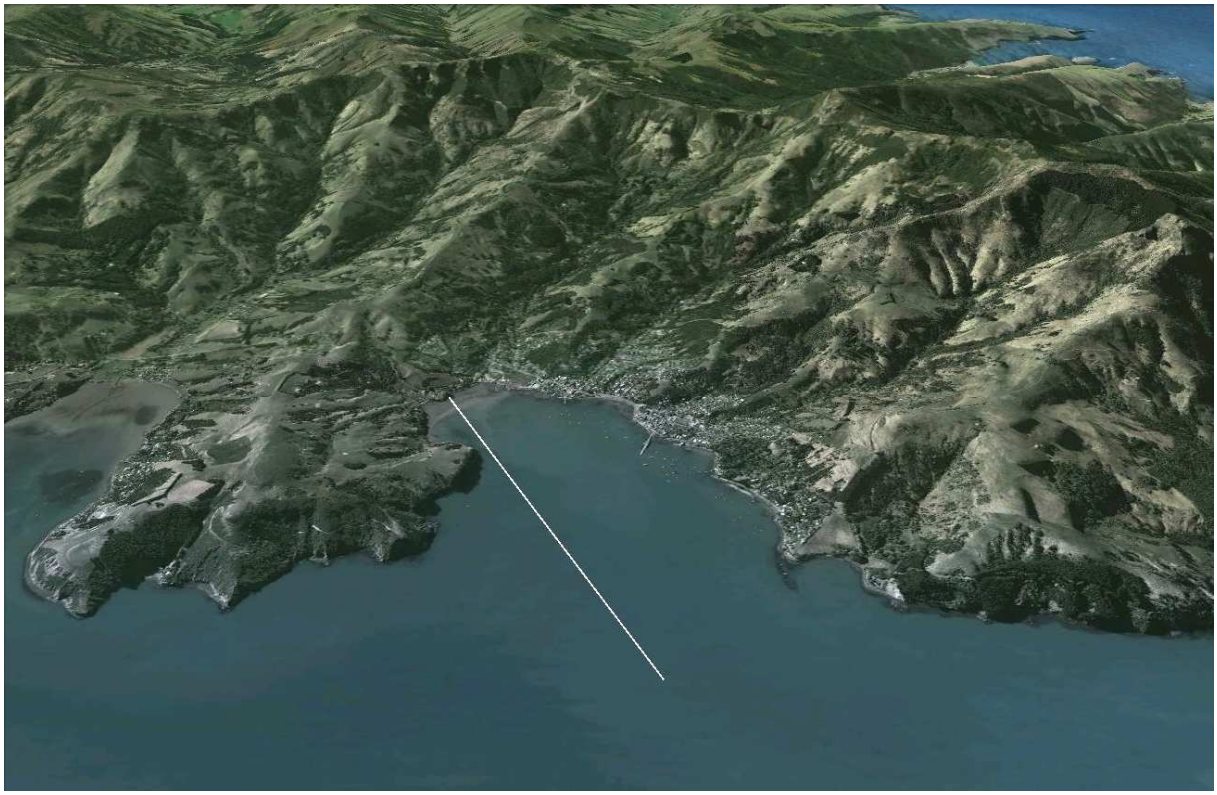

Authors/Contributors:
Rob Bell
Glen Reeve
Chris Palliser

For any information regarding this report please contact:

Rob Bell
Programme Leader: Hazards & Risk
Coastal and Estuarine Processes Group
+64-7-856 1742
rob.bell@niwa.co.nz

National Institute of Water & Atmospheric Research Ltd
Gate 10, Silverdale Road
Hillcrest, Hamilton 3216
PO Box 11115, Hillcrest
Hamilton 3251
New Zealand

Phone +64-7-856 7026
Fax +64-7-856 0151

NIWA Client Report No:	HAM2014-027
Report date:	April 2014
NIWA Project:	BEC14201

Cover: Oblique view of Akaroa looking east annotated with the 2.5 km outfall line. [Credit: DigitalGlobe and Google Earth]

Contents

Tables

Figures

Reviewed by

Scott Stephens

Approved for release by

Andrew Swales

Formatting checked by

Executive summary

The present wastewater treatment plant (WWTP) is located south of Akaroa township at the end of Beach Road and discharges treated wastewater through a 100-m long outfall at a 5.9 metre depth off Redhouse Bay under consent CRC071865. Christchurch City Council (CCC) commissioned the Akaroa Wastewater System Project in late 2013 as part of a long-term strategic plan on water and wastewater management in the Akaroa area. The purpose of the project is to modify and upgrade the wastewater reticulation system, and construct a new treatment process plant and harbour outfall.

CH2M Beca Ltd have been engaged by CCC to undertake investigations, obtain consents/permits and commission a new WWTP to the north of Akaroa township including upgrades of the trunk sewer main and a new outfall into Akaroa Harbour. CH2M Beca have sub-contracted NIWA to undertake harbour modelling and assess public-health risk associated with the proposed new outfall.

The Scope of the Services provided by NIWA as contracted by CH2M Beca in December 2013 covered the following aspects:

- Deploying a current meter and tide gauge for 32 days (including harbourmaster approvals for the current-meter deployment).
- Preparing a hydrodynamic model of Akaroa Harbour and a dispersion model of the wastewater discharges from a specified new outfall diffuser.
- Deriving cumulative distributions of virus surrogate concentration-reduction factors at up to twelve[1] sites for the quantitative microbial risk assessment (QMRA).
- Preparing a report on the hydrodynamic and dispersion modelling.
- Undertaking a QMRA to assess the potential human health risk of the wastewater discharge from the proposed Akaroa WWTP via the proposed harbour outfall.
- Preparing a report summarising the assessment of public-health effects arising from the QMRA, for inclusion as an appendix to the overall Assessment of Environmental Effects report.

This Report covers the first four aspects, while the last two tasks are covered in a separate NIWA report (McBride, 2014).

The main modelling components described in this Report are the:

1. Development of the 2-dimensional curvilinear mesh hydrodynamic model for Akaroa Harbour.
2. Calibration and verification of the hydrodynamic model based on existing available water level data and recently collected current-meter data.

[1] Was changed later in the project to 14 sites

3. CORMIX near-field mixing model to predict initial dilution in the vicinity of the proposed outfall diffuser in the middle of the Harbour (2.5 km outfall).

4. Far-field hydrodynamic\dispersion model (Delft2d) for simulating far-field physical dispersion achieved at 14 specified sites within Akaroa Harbour.

5. Processing of virus dilutions (near-field and far-field) and inactivation at the 14 selected sites to generate cumulative distribution functions of the predicted frequency of occurrence of virus concentrations (based on an effluent level of 1 virus/L) as input to the QMRA process.

Summary of results

Some key findings from the 1-year model simulations:

- Initial dilution within the vicinity of the proposed outfall diffuser is one of the main contributors towards reducing virus concentrations at all of the coastal sites, followed closely by microbial inactivation, especially the more remote sites with long plume travel-times, while the smallest reduction is from subsequent dispersion (which incorporates slow overall flushing from the Harbour).
  - The median initial dilution is around 1480-fold, but decreases as the effluent discharge increases or the current velocity drops. Plume mixing with the receiving waters is much more efficient for lower discharges into faster current speeds.
  - Mostly, the far-field physical dilution factor is small at around 2–3 fold dilution, as it also includes the moderating effect of the harbour-wide flushing characteristics for the semi-enclosed Harbour (where a dynamic equilibrium is reached between the effluent discharge load (when modelled as a conservative tracer) and the volume exchanged each tide with the Canterbury Bight waters).
  - Average virus inactivation over the entire year ranged in a wide band from a 1.3-fold reduction at the middle Harbour site 14–MHb 160 m north of the proposed diffuser, 5-6 fold reduction covering sites 2-6 in French Bay, up to nearly 100-fold reduction for upper-harbour sites. These reductions due to microbial inactivation are directly reflected in the plume travel-time to each site, given the same hourly solar radiation (measured at the Akaroa EWS) was input to the inactivation algorithm for all sites.
- The approach of dis-aggregating the far-field physical mixing processes for a non-decaying substance and later factoring in microbial inactivation for viruses during post-processing is likely to be conservative by underestimating physical far-field dilutions at each site, particularly sites closer at hand to the outfall in the middle Harbour.
- The combined total dilution and inactivation achieved at all sites was slightly lower in winter (leaving aside the influence of wet-weather effluent flows) than in summer, even though the dry-weather effluent discharge rates are smaller (producing higher initial dilutions). This is due to the substantially lower microbial inactivation in winter.

- Based on median values, Site 14–MHb in the middle of the Harbour (160 m north of the proposed diffuser site) understandably produces the lowest total dilution plus inactivation of around 500-fold. For the other sites, total dilution plus inactivation over the summer-bathing season ranges from a median of 860-fold dilution at site 7–ExW (near the existing outfall south of Akaroa township) up to a 1.1×10^7 fold reduction at site 12–FFB in the upper Harbour (French Farm Bay). The lower dilutions that would be achieved at site 7–ExW (compared with the upper Harbour sites e.g., site 12), would arise from the eastern periphery of the dispersing ebb-tide plume sometimes brushing this area. However the total dilution and inactivation at site 7–ExW from the proposed outfall scheme will be substantially higher than that presently being achieved in this area by the existing short outfall 150 m to the north of site 7 (Figure 5-2) with the discharge from the present WWTP.
- Both upper-harbour sites 12–FFB and 13–TaB are predicted to yield very large total dilutions plus inactivation, primarily due to the cumulative microbial inactivation of nearly 100-fold that will occur over the long travel times of over 8 days for the very dilute plume to reach these sites.

Final deliverables

The final stage was to invert the total dilution plus inactivation to a concentration-reduction factor to produce cumulative distribution functions (CDFs) of normalised concentrations (scaled to an effluent concentration of 1 virus/L) from the 1-year time series. The more than 35,000 15-minute values at all of the 14 specified sites of interest were sorted into ascending order and percentile values calculated to define the cumulative distribution functions.

For the QMRA analysis, Graham McBride (NIWA) was supplied these cumulative distribution functions for each of the selected sites, which were normalised to an effluent concentration of 1 virus/L and only require multiplying by a final-effluent virus concentration in viral units per litre, to get concentrations at each site.

1 Introduction

1.1 Background

The present wastewater treatment plant (WWTP) south of Akaroa township is at the end of Beach Road (Figure 1-1) and discharges treated wastewater through a 100-m long outfall at a 5.9 metre depth off Redhouse Bay under consent CRC071865. Christchurch City Council (CCC) commissioned the Akaroa Wastewater System Project in late 2013 as part of a long-term strategic plan on water and wastewater management in the Akaroa area. The purpose of the project is to modify and upgrade the wastewater reticulation system, and construct a new treatment process plant and harbour outfall.

CH2M Beca Ltd have been engaged by CCC to undertake investigations, obtain consents/permits and commission a new WWTP to the north of Akaroa township including upgrades of the trunk sewer main and a new outfall into Akaroa Harbour.

The CH2M Beca project team includes sub-contractors such as Cawthron Institute (harbour water quality and ecology), OCEL Consultants NZ Ltd (harbour outfall design and construction) and NIWA (harbour modelling and public-health risk).

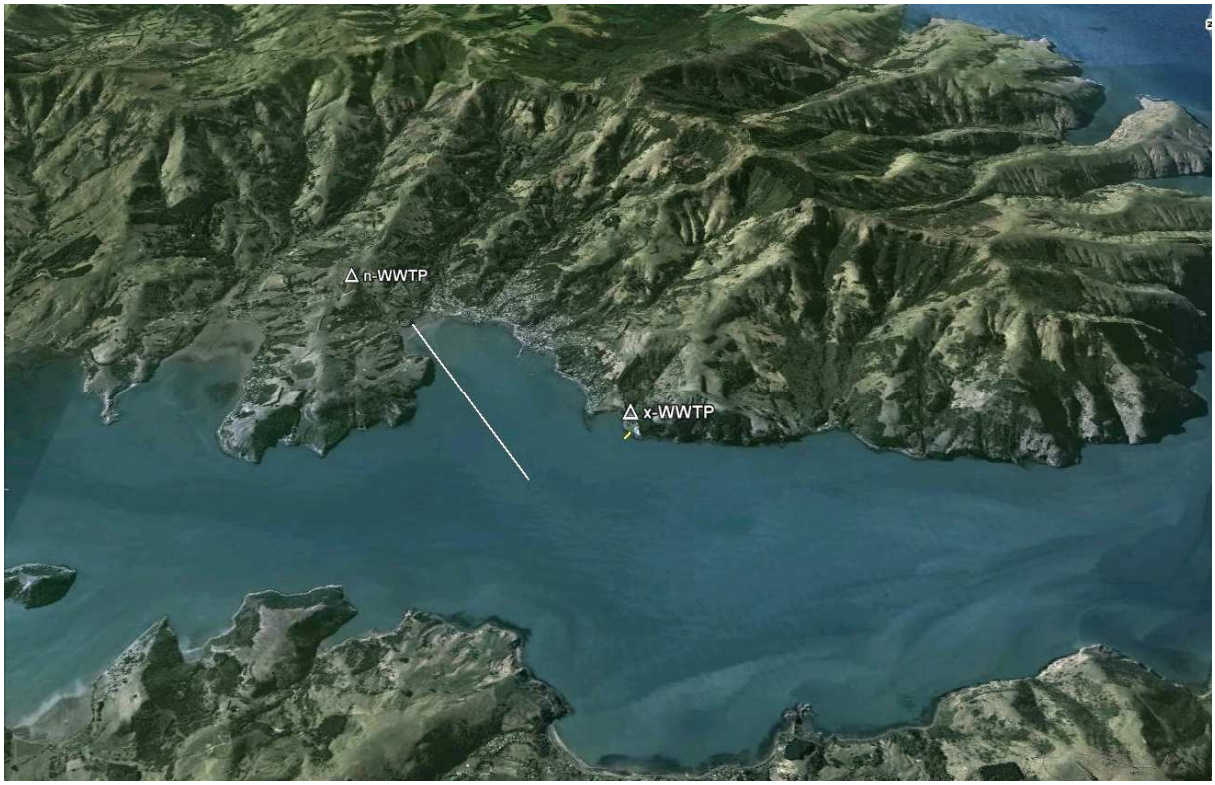

Figure 1-1: Akaroa Harbour and location of existing WWTP (x-WWTP) and short 100 m outfall (yellow) and proposed WWTP site (n-WWTP) and 2.5 km long outfall (white). Viewpoint to the east. [*Background image*: TerraMetrics, DigitalGlobe, Google Earth]

1.2 Scope of services

The Scope of the Services provided by NIWA as contracted by CH2M Beca in December 2013 covered the following aspects:

- Deploying a current meter and tide gauge for 32 days (including harbourmaster approvals for the current-meter deployment).
- Preparing a hydrodynamic model of Akaroa Harbour and a dispersion model of the wastewater discharges from a specified new outfall diffuser.
- Deriving cumulative distributions of virus surrogate concentration-reduction factors at up to twelve[2] sites for the quantitative microbial risk assessment (QMRA).
- Preparing a report on the hydrodynamic and dispersion modelling.
- Undertaking a QMRA to assess the potential human health risk of the wastewater discharge from the proposed Akaroa WWTP via the proposed harbour outfall.
- Preparing a report summarising the assessment of public-health effects arising from the QMRA, for inclusion as an appendix to the overall Assessment of Environmental Effects report.

1.3 Overview of this report

This modelling report describes the following:

1. Development of the 2-dimensional curvilinear mesh hydrodynamic model for Akaroa Harbour (covering the coloured region in Figure 1-2).
2. Calibration and verification of the hydrodynamic model based on existing available water level data and recently collected current-meter data.
3. CORMIX near-field mixing model to predict initial dilution in the vicinity of the outfall diffuser.
4. Far-field hydrodynamic\dispersion model (Delft2d) for simulating physical dispersion achieved at 14 specified sites (1–14) within Akaroa Harbour (Figure 1-2).
5. Processing of virus dilution and microbial inactivation for the 14 specified sites to generate cumulative distribution functions of the predicted frequency of occurrence of virus concentrations (based on an effluent level of 1 virus/L) as input to the QMRA process.

A companion NIWA report (McBride, 2014) covers the public-health aspects of the scope for services, based on a QMRA process.

[2] This was changed later in the project to 14 sites

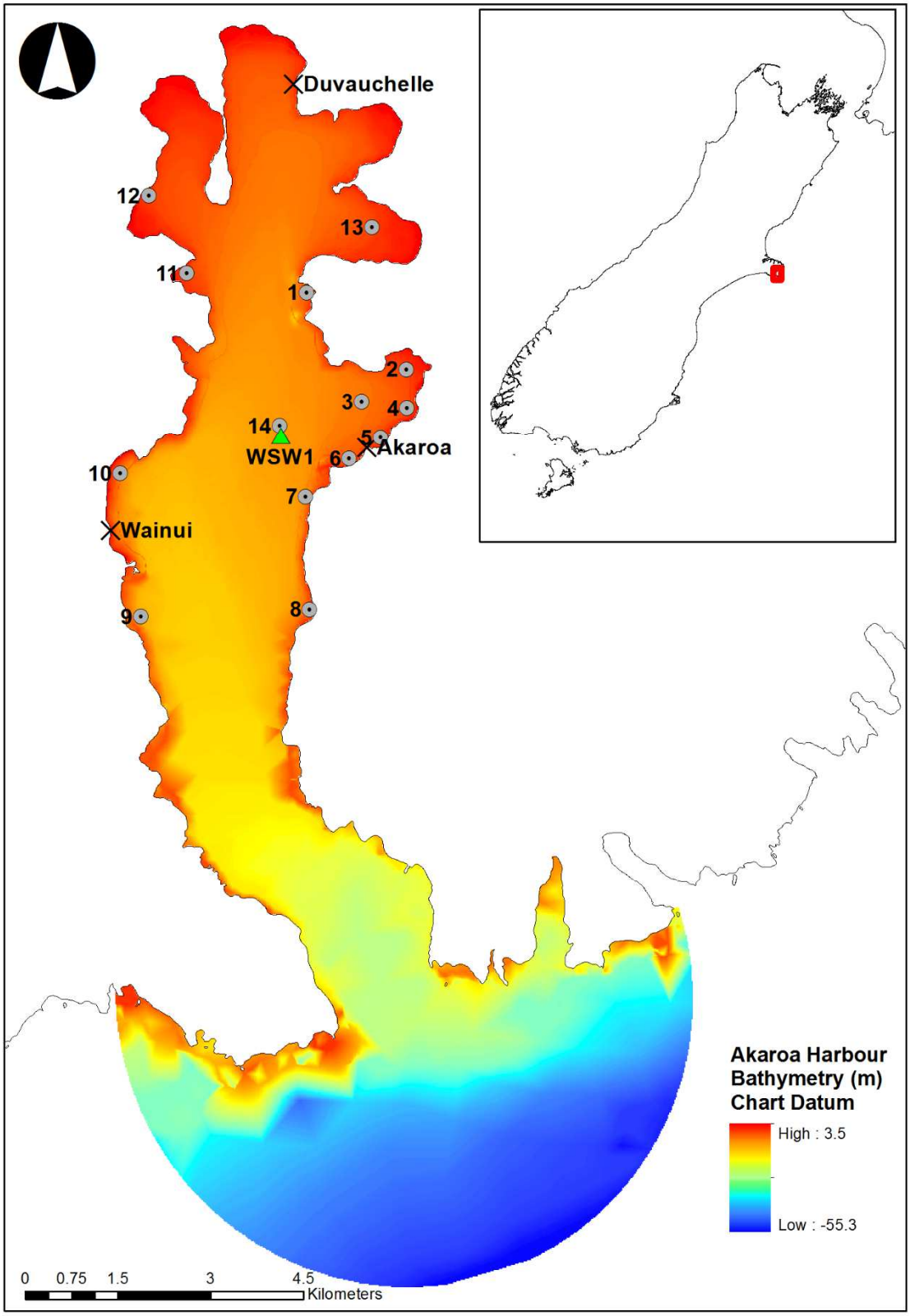

Figure 1-2: Akaroa Harbour, Banks Peninsula. Grey circles indicate the specified sites for which dilutions were processed, X mark tide-gauge sites, WSW1 is the proposed outfall diffuser site and seabed heights (m) are relative to Chart Datum (lowest low tide). [*Bathymetry source*: Land Information NZ and Environment Canterbury/University of Canterbury]

2 Climate and oceanographic datasets

2.1 Background oceanography (previous studies)

Akaroa Harbour occupies a drowned crater in an extinct volcanic complex on the southern side of Banks Peninsula, being nearly 17 km long with a predominantly north-south orientation (Heuff et al. 2005).

The Harbour entrance is 1.6 km wide at its narrowest section off Te Ruahine Point and up to 25 m deep (below Chart Datum). The Harbour gradually widens and becomes shallower to the north. At the proposed outfall diffuser site in the middle of the Harbour, the depth is around 8 m below Chart Datum. Depths shallow further terminating in intertidal flats at the head of five embayment's at the northern end of the Harbour.

The tide range varies from 1.2 to 2.3 m on average neap and spring tides respectively (LINZ, 2013). The present-day mean sea level (MSL) is around 1.5 m above Chart Datum, based on the 2008 hydrographic survey (LINZ, 2009; LINZ, 2013). Another estimate of MSL of 1.58 m was obtained by Goring (2008) for a different period – but both gauge deployments were for relatively short periods of a few months.

Heath (1976) presented some of the key hydrographic characteristics of Akaroa Harbour:

- surface area of the Harbour at high tide = 44 km^2
- surface area of mud flats exposed at low tide as 2 km^2 (~4% total area)
- Harbour volume at low water spring as 5×10^8 m^3
- tidal prism (tidal volume in and out) each neap tide = 6.5×10^7 m^3 (13% of low water spring-tide volume)
- tidal prism (tidal volume in and out) each spring tide = 8.1×10^7 m^3 (16% of low water spring-tide volume)
- basin catchment area = 200 km^2 (including the Harbour)
- average annual freshwater run-off of only 2 m^3/s, most of which occurs in winter (July run-off is 6 m^3/s)
- the Harbour residence time was calculated by Heath (1976) using two different analytical methods. Assuming complete export offshore of the harbour spring-tide prism for each spring-tide cycle, a low estimate was derived of only 3.7 days. At the other extreme, assuming exchange of the harbour waters only occurs via replacement of the catchment freshwater run-off, then an estimate of 7.9 years was obtained (due to the small inflow). Neither of these estimates provides a realistic residence time for the Harbour, which can now be achieved using the hydrodynamic model set up for this Project (see Section 5.2.1).

Hicks and Marra (1988) measured peak flood-tide and ebb-tide current speeds off Green Point (reef just north of the present outfall) of 0.18 and 0.20 m/s respectively. Elsewhere in the middle harbour and French Bay, their measured current speeds were generally less than

0.1 m/s. Velocities towards the Harbour entrance are higher – up to 0.45 m/s from the 1998 ADP deployment (Heuff et al. 2005).

2.2 Winds

Wind measurements are available from the following stations or weather models in the region around Akaroa Harbour, however only the Akaroa EWS and the EcoConnect weather-model output from the 12 km grid have records beyond a year.

- Main environmental weather station (EWS) at Akaroa operated by NIWA since November 2008 (Agent #36593).
- Temporary Christchurch City Council weather station on the proposed WWTP site (CCC WS).
- NIWA EcoConnect weather model wind fields for Banks Peninsula at 12 km resolution.
- NIWA EcoConnect weather model wind fields for Banks Peninsula at 1.5 km resolution.

The two wind stations (EWS and CCC WS) are shown in Figure 2-1.

Figure 2-1: Location of wind, tide-gauge and ADP current-meter stations in Akaroa Harbour. [*Background image*: DigitalGlobe, Google Earth].

The Akaroa EWS wind dataset spans almost 5 years, having been established in November 2008. However, the outputs from the NIWA 12 km resolution EcoConnect climate model of Banks Peninsula (1 year of data for 2013) and the new 1.5 km high-resolution EcoConnect model outputs show that winds within Akaroa Harbour basin are strongly influenced by local topography of the surrounding hills and valleys. Winds measured during the 1-month

acoustic Doppler profiler (ADP) current-meter deployment are shown in Figure 2-2 to Figure 2-4.

The wind-frequency rose from the elevated CCC weather station at the proposed WWTP site (which approximately matches with the finer 1.5 km EcoConnect grid output for that location) suggest that winds offshore in the Harbour mainly exhibit an approximate north-south direction down the axis of the Harbour. This was also the pattern found by Heuff et al. (2005) from a wind station temporarily deployed in 1998 at the southern end of Wainui Bay.

Heuff et al. (2005) also established a relationship between the Le Bons Bay automatic weather station (AWS) on the eastern tip of Banks Peninsula operated by the Met Service and the local winds measured in the Harbour. However, we weren't able to utilise this relationship to Harbour winds as we could not secure Le Bons AWS data for 2013 from Met Service for consultancy applications.

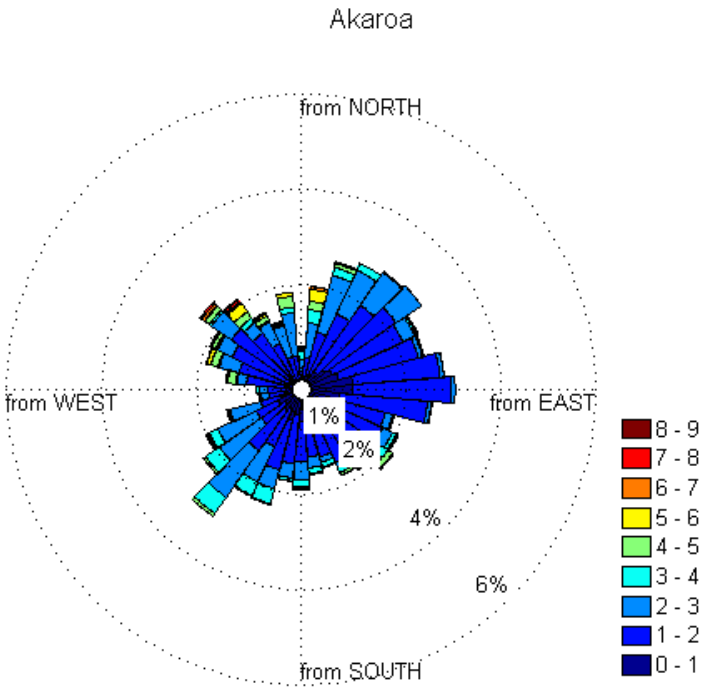

Figure 2-2: Akaroa weather station (EWS) wind rose sampled for the 1 month ADP current-meter deployment period 13-Nov to 18-Dec 2013.

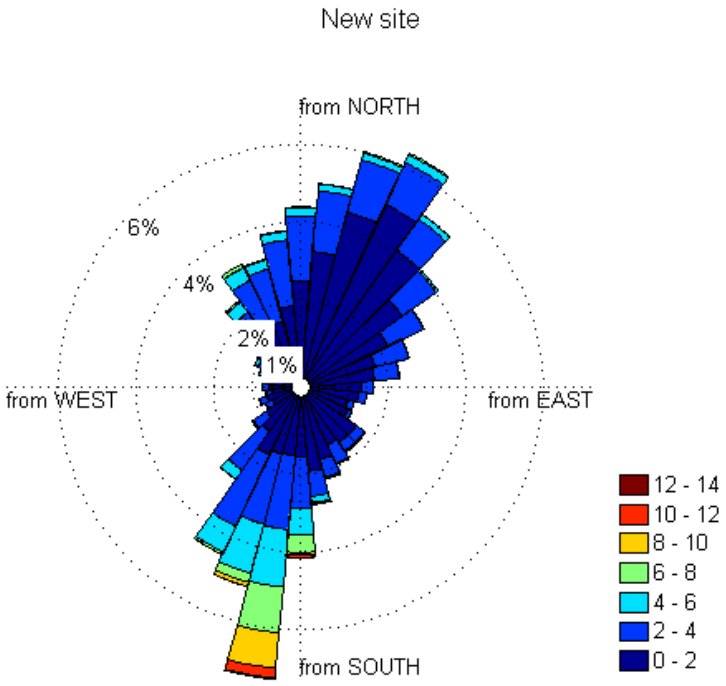

Figure 2-3: Christchurch City Council weather station (CCC WS) sampled for the 1 month ADP current-meter deployment period 13-Nov to 18-Dec 2013.

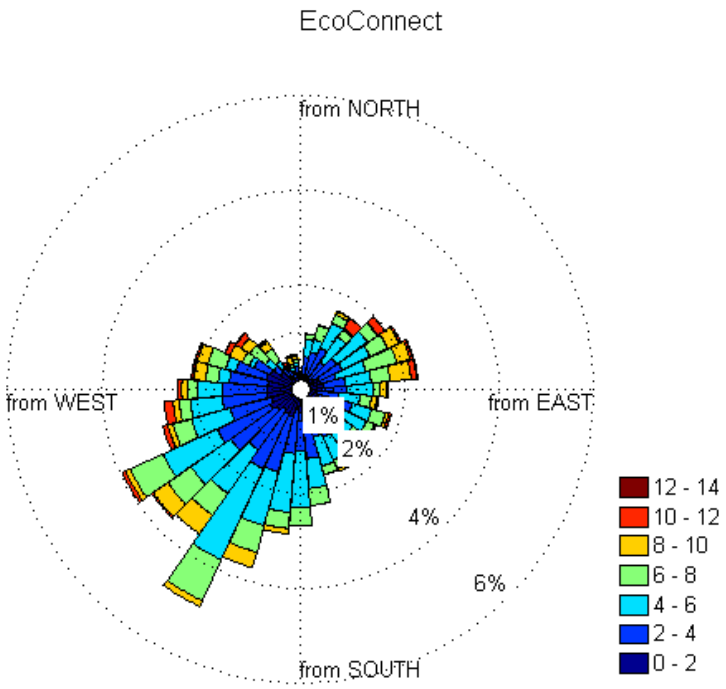

Figure 2-4: EcoConnect wind hindcast from the 12 km grid sampled for the 1 month ADP current-meter deployment period 13-Nov to 18-Dec 2013.

Winds from the east or west quarters are diminished by the sheltering effect of the surrounding terrain, but also include local effects from air drainage down adjacent valley systems. Most of the stronger storms have been associated with southerlies and tend to be more frequent in winter.

Given the local channelling of winds along the main axis of Akaroa Harbour (mostly south or north), the wind record from the 1-year 12 km EcoConnect hindcast for 2013 was used as the starting point for establishing a wind time series for the hydrodynamic modelling. A hybrid wind time series was then developed by replacing the east-west component winds from the EcoConnect 12 km coarser forecast re-analysis, with measured east-west winds from the Akaroa EWS to capture more accurately local cross-winds experienced across the Harbour in the area around the proposed outfall. This hybrid wind time series was then applied uniformly across the entire model domain (shown by coloured area in Figure 1-2). This approach may not entirely capture the complex topographic steering of winds throughout Akaroa Harbour at the local scale. However, the simulated currents from the hydrodynamic model and the ADP current-meter measurements were not overly sensitive to variability in winds and are more dominated by the tide (discussed further in Section 4.3).

2.3 Tide heights

To enable tides to be predicted forward in time, tidal constituents (sine wave amplitudes and phases) of the main tidal components that make up the observed tide can be extracted from a time series of tide heights – provided the data record is at least 32 days and preferably longer.

This approach was taken as tide data for the ADP current-meter deployment was only available from one site in the Harbour at Akaroa wharf (via a temporary NIWA installation). But tidal measurements were also available[3] from temporary tide gauges at Duvauchelle (north end) and Wainui (western side) for a 32-day period from 28-Feb to 1-Apr in 2008 and a longer overlapping gauge record at the Akaroa wharf from 24-Oct 2007 to 1-Apr 2008.

Tidal constituents extracted from measured records for each of the two sites (Duvauchelle and Wainui) were used to generate “observed” tide-height time series for the 2013 year-long simulation period for the hydrodynamic model, which could then be compared with modelled tide height results. The three major tidal constituents: M_2 (lunar twice-daily tide); S_2 (solar twice-daily tide), and N_2 (lunar elliptical orbit twice-daily tide) at these sites are listed in Goring (2008).

Tidal heights were required on the open-sea boundary of the hydrodynamic model (Figure 1-2) to drive tidal flows within the model domain. Tidal constituents from a tidal model of New Zealand’s EEZ by Walters et al. (2001), which is used as the Tide Forecaster on NIWA’s web site, were selected for a few locations along the open-sea boundary of the Akaroa model grid set up for this project (Section 3.3). These sets of 13 tidal constituents were used to generate a time series of tidal heights for the 1-year simulation period spanning 2013, which were interpolated smoothly around the open-sea boundary of the model domain.

To provide for a wide variety of environmental conditions, the 1-year model simulation also included storm surges and set-downs in sea level due to low-pressure weather systems and

[3] These datasets were obtained from Mulgor Consulting Ltd (Derek Goring) for a CCC project in 2008 to establish a reliable vertical drainage datum and set mean high water spring (MHWS) marks for Akaroa Harbour

anti-cyclones respectively. Given storm-surge and set-down generally occurs similarly across the entire Canterbury Bight, post processing of the Timaru water level record for 2013 was undertaken to extract the storm surge and set-down component of the sea level record. Tides locally tend to ride on the back of these higher or lower sea levels which occur over wide spatial and temporal scales of a shelf system such as the Canterbury Bight under varying weather systems. Therefore, the 2013 tidal predictions for Akaroa Harbour entrance were added to the low-pass filtered storm surge record from Timaru for the same year.

2.4 Solar radiation and water clarity

Microbial species found in wastewater, such as bacteria and viruses are, following discharge to the marine environment, eventually rendered inactive by solar radiation (particularly the short wavelength part of the light spectrum) and to a lesser extent by changes in temperature and salinity and predation by micro-fauna.

Solar radiation is routinely monitored by the NIWA at their automatic weather station at Akaroa EWS (Agent #36593). Solar radiation is the energy from the Sun that is received on the Earth's surface per square metre and accumulated over each hour, measured in MJ/m^2.

Figure 2-5 shows the seasonal and diurnal variability in hourly solar radiation from the Akaroa EWS station for the model simulation period 1 January 2013 to 1 January 2014. As expected, peak solar insolation occurs over summer and is lowest in winter. This data was used to determine the reduction in concentration of viruses due to solar inactivation, over and above physical dilution processes (see Appendix 1).

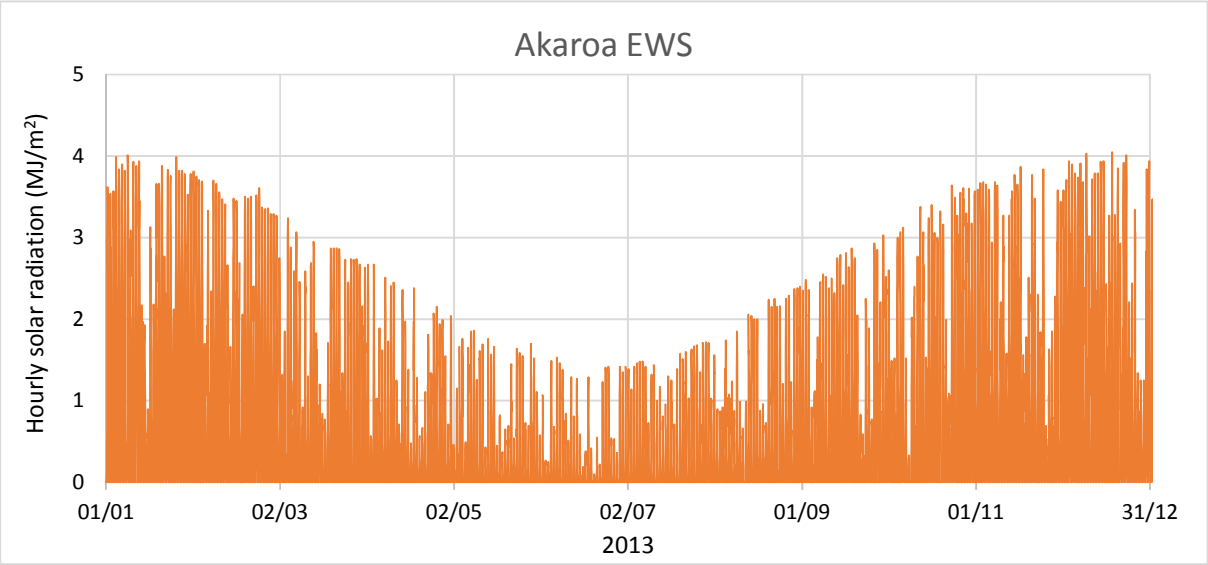

Figure 2-5: Hourly solar radiation measured at the Akaroa EWS. [*Source*: NIWA Climate Database]

Water clarity in the region of the discharge also determines how far solar radiation is transmitted down into the water column, particularly the short ultra-violet (UV) and short visible wavelengths which can be attenuated relatively quickly below the water surface.

No data was available on UV and short-visible wavelength transmission in Akaroa Harbour waters over the course of the year-long 2013 simulation. Figure 2-6 from Bell et al. (1992) shows measurements of attenuation at various UV and short-visible wavelengths 2 m below

the surface at two sites in the waters of Lyall Bay. Attenuation can be expressed both as L_{90} (the depth at which 90% attenuation of that wavelength occurs) and an attenuation coefficient in attenuation of light intensity per metre. The optical water typologies for ocean (II, III) and coastal waters (1–9) from Jerlov (1976) are also overlain on Figure 2-6. Lyall Bay waters of Cook Strait are relatively clear, with substantial penetration of UV and short-visible wavelengths e.g., for UV-A 340 nm wavelength, which is relevant for microbial inactivation, the attenuation coefficient is around 0.46 m^{-1} or an L_{90} of 5 m before light at that wavelength is attenuated by 90%.

In Akaroa Harbour, the waters are not likely to be as clear as Lyall Bay waters, but given it is a deeper sound-like water body, optical type 1 Coastal waters are likely to be relevant. On this premise, the attenuation coefficient for Akaroa Harbour was selected to be ~0.10 m^{-1}, or a L_{90} of 2.3 m for 340 nm wavelength. In any case, the inactivation rate is less sensitive to this attenuation parameter than the day-to-day variability in solar radiation.

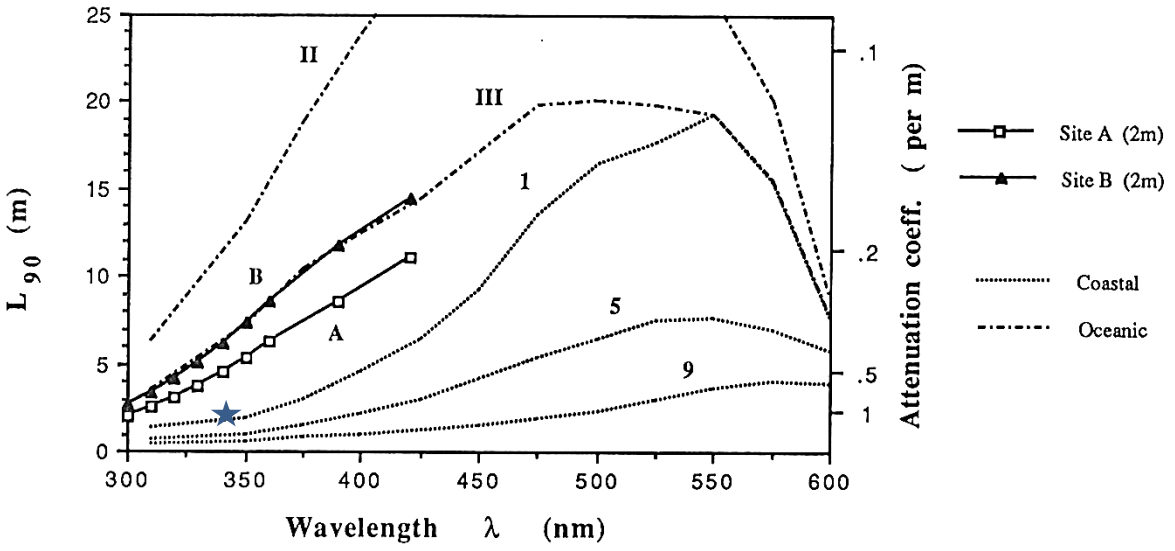

Figure 2-6: Attenuation of UV and short-visible solar radiation in ocean and coastal waters. Sites A and B are detailed measurements from clear waters off Lyall Bay (Cook Strait), with an estimate of attenuation for Akaroa Harbour shown by the star for 340 nm wavelength. Attenuation profiles for various classes of the optical quality waters for coastal waters around the world (types 1–9; with type1 being the clearest) and clearer oceanic waters (types II, III) shown to provide context. [*Source*: Bell et al. (1992)]

3 Numerical models

3.1 Models used

To encompass all the outfall plume dilution processes at different spatial and time scales including the microbial inactivation due primarily to solar radiation, three different models were applied to cover the three phases that contribute to a reduction in virus concentrations by the time the dilute plume reaches each of the 14 specified sites:

- *Initial dilution* occurs in the immediate vicinity of the outfall diffuser (within approximately 50 m of the diffuser in the Akaroa situation) due to buoyancy and shear forces on the jets emanating from each diffuser port as the lighter freshwater-based effluent rises towards the surface and mixes with the adjacent marine waters. These near-field processes were modelled using CORMIX, which is described in section 3.2.
- *Subsequent dispersion and Harbour mixing* includes physical mixing processes that contribute to the further dilution of the plume after the initial-dilution phase until it reaches a site of interest. In a harbour, it also includes the accounting for harbour residence or flushing times, particularly if the effluent constituent of interest exhibits conservative (non-decaying) or slow-decay behaviour in the receiving waters. This phase was modelled using Delft2d.
- *Microbial inactivation* of microbial species found in wastewater, such as bacteria and viruses are, following discharge to the marine environment, is primarily caused by solar radiation (particularly the short wavelength end of the light spectrum) and to a lesser extent by changes in temperature and salinity and predation by micro-fauna. This phase was modelled using the inactivation algorithm in Appendix 1 based on solar radiation measurements at the Akaroa EWS.

A detailed description and the set-up of each of these models is provided below.

3.2 Near-field mixing model

A discharge of wastewater through the outfall diffuser into saline marine waters, rises towards the surface due to the buoyancy of the lighter-density freshwater, entraining saline waters within the plume leading to substantial dilution of the wastewater known as initial dilution. The momentum of the jets that exit the ports in the diffuser also create shear stresses on the edge of the individual plumes, also causing entrainment and mixing with the ambient saline waters. The initial dilution process is illustrated in Figure 3-1.

Near-field initial dilution of the outfall discharge were determined by the CORMIX model (version 8.0GTD), an internationally accepted plume model originally developed by the U.S. Environmental Protection Agency (Jirka et al. 1991).

Doneker & Jirka (2012) describe the near-field as the region of receiving water where the initial discharge jet characteristics of momentum flux, buoyancy flux and outfall geometry influence the jet or plume trajectory and mixing of an effluent discharge. Thereafter, the subsequent dispersion and dilution phase is when the local environmental processes

including current velocity, circulation patterns, winds and ambient turbulence influence the behaviour and advection of the plume.

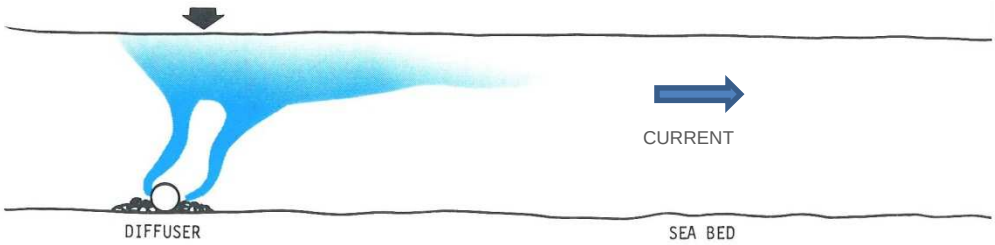

Figure 3-1: Schematic side view of buoyant plumes from an outfall diffuser.

CORMIX is primarily a static near-field model i.e., it takes a snapshot in time of what happens to the discharged wastewater in the near-field around the diffuser. This is satisfactory since the times taken for the effluent to mix in the near-field are relatively short. CORMIX employs a rule-based expert system to screen input data and select the most appropriate hydrodynamic module within CORMIX to simulate the physical mixing processes within a given discharge environment.

As CORMIX is limited to current velocities across the diffuser above a threshold of around 0.03 to 0.05 m/s, the initial dilutions for slower current speeds were supplemented by the use of the DIFFUSER algorithm (Williams, 1985 and Wood et al. 1993) to calculate still-water initial dilutions, which generally only occur for short periods when the tidal current changes direction. DIFFUSER calculates minimum plume-centre initial dilutions, so these we multiplied by a factor of 1.3 to convert to plume-averaged initial dilutions to match the output from CORMIX.

3.2.1 Outfall diffuser

After consideration of various outfall alignments in French Bay, CH2M Beca and OCEL consultants provided the west-south-west alignment shown in Figure 3-2, with the short diffuser to be located between WSW1 (2.5 km offshore) and WSW2 (2.9 km offshore) in water depths of 9.5 m and 10.3 m respectively below mean sea level. For comparison, the present 100-m outfall is also shown in Figure 3-2.

A diffuser is the short section at the end of an outfall pipe with small ports (outlets) that discharge the treated wastewater – usually in a horizontal direction aligned with the predominant flow directions to maximise the initial dilution (see example in Figure 3-3).

In collaboration with CH2M Beca and OCEL Consultants, the specimen design for the diffuser to input into CORMIX and DIFFUSER was determined to consist of 3 risers separated by approximately 6 m, with each riser comprising two oppositely-directed duck-bill valves aligned with the prevailing tidal flow, making 6 ports altogether.

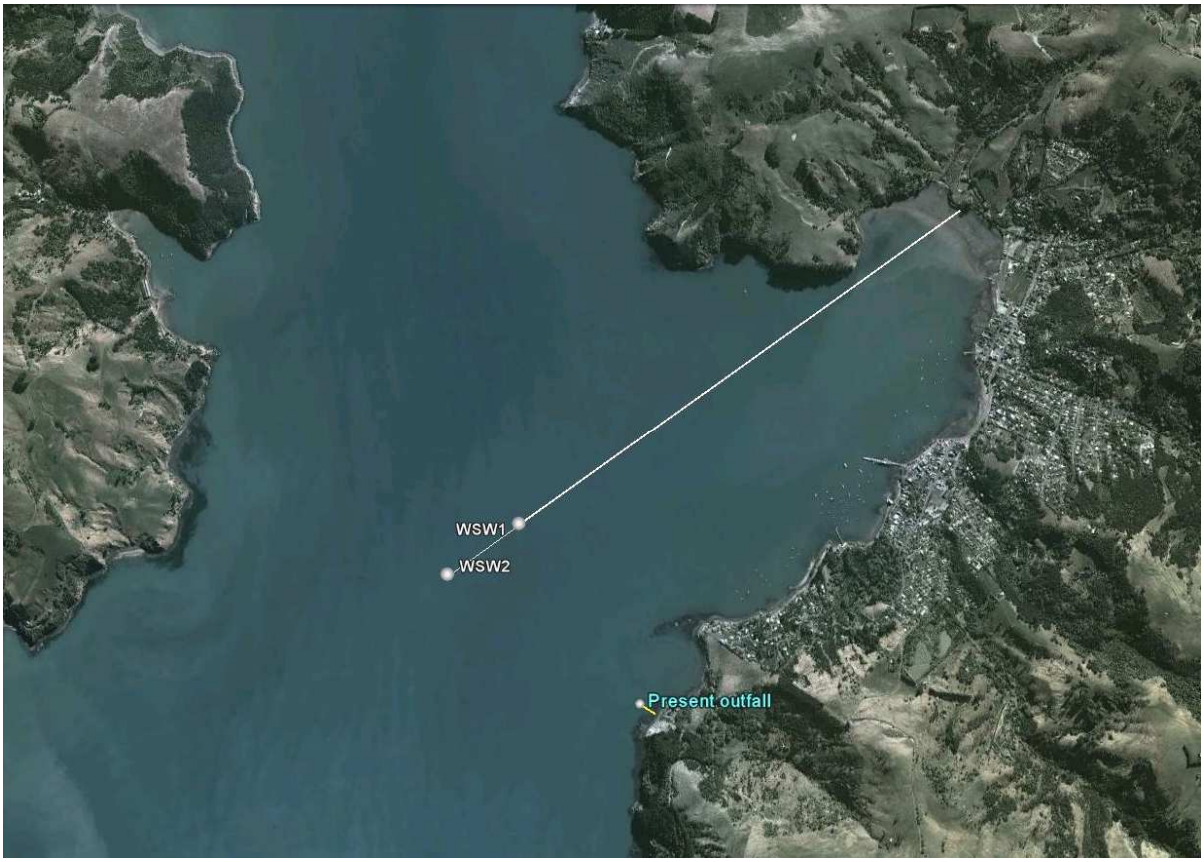

Figure 3-2: Proposed outfall alignment and the existing 100 m outfall in Akaroa Harbour. WSW1 (2.5 km) and WSW2 (2.9 km) mark the start and end of sites considered for the short diffuser section.

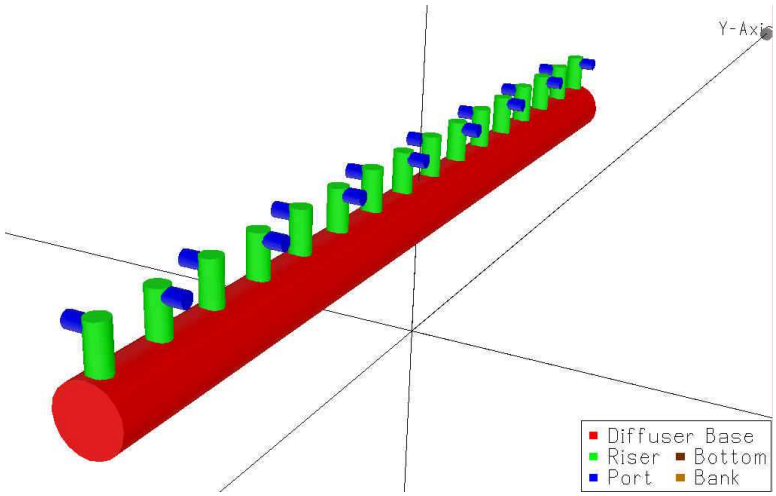

Figure 3-3: Schematic of an outfall diffuser with risers. Ports can be alternate on each riser, or for the specimen design for Akaroa, alternate ports would be positioned on each of 3 risers to make 6 ports in total. [*Source*: CORMIX web site: http://www.cormix.info/methodology.php]

Duck-bill valves are made from semi-flexible rubber, transitioning from a circular flange on the riser pipe out to a flat bill section that remains closed if there is no effluent flow, but opens progressively with an elliptical cross-section as the effluent discharge increases. The hydraulic performance of the valves was based around a PROCO 75 mm duck-bill valve of standard weight[4] and the diffuser was approximated using circular port areas that are equivalent to the same cross-sectional flow area of the duck-bill opening for any specific effluent discharge. So for each particular effluent discharge, a 6 port alternate-side diffuser with 3 riser pipes was determined with a particular port area, ranging from equivalent circular port diameters of 21 mm (1.7 L/s minimum flow) up to 57 mm (peak wet-weather flow of 65 L/s).

3.2.2 Input parameters for CORMIX

Table 3-1 lists the parameters used as inputs to the initial dilution model CORMIX and how they were obtained. A smaller subset of these parameters were also used for the DIFFUSER algorithm.

These parameters were obtained from information supplied by CH2M Beca, the hydrographic chart NZ6324 (LINZ, 2009), the Delft2d model (range of current speeds) and other sources noted in Table 3-1.

Multiple simulations of CORMIX (or DIFFUSER for still-water) were then pre-computed for a series of combinations of:

- wastewater discharge rates ranging from 1.7 L/s to 65 L/s
- current speed across the diffuser ranging from 0.0 to 0.15 m/s in increments of 0.01 m/s
- tidal heights were extracted from the 1-year Delft2d simulation at the outfall site and assigned to one of three classes: (low water) (mid-tide) (high tide)
- seasons (winter and summer) for wastewater and receiving water densities.

As a scoping exercise, the DIFFUSER algorithm was used to compare initial dilutions in still-water (the worst case) at the two sites WSW1 and WSW2 on the proposed outfall alignment in Figure 3-2. Given the modest 8-14% increase in initial dilution that would be achieved at the outer diffuser site (WSW2) for a 16% longer outfall out over a more gently sloping part of the Harbour seabed, the more complex time-consuming CORMIX simulations were only undertaken on a diffuser at site WSW1 (2.5 km outfall), as directed by the CH2M Beca project team.

The offshore terminus of a 2.5 km outfall was therefore taken to be at WSW1 which in WGS-84 coordinates is at -43.8104° N and 172.9388° E.

[4] NIWA does not specifically endorse this particular product – simply using it as an example for the specimen diffuser design.

Table 3-1: Input parameters based on a diffuser at WSW1 used for the initial dilution models CORMIX and DIFFUSER.

Inputs	Variable	Data	Notes
Wastewater	Discharge rate through diffuser (m^3/s)	0.0017, 0.0034, 0.0117, 0.0300, 0.0475, 0.0650 in increments of 0.10[a]	Minimum = 0.0017, future 2041 winter ADWF = 0.0034, future 2014 peak summer day = 0.0117, and PWWF = 0.0650 (R. Bouman, CH2M Beca, pers. com.). Note: 0.0300 and 0.0475 used for interpolation up to PWWF.
	Density of effluent (kg/m^3)	winter = 1000.25 summer = 998.74	Based on effluent temperatures of 10°C and 20°C in winter and summer respectively, and salinity between 0.5–0.9 psu (R. Bouman, CH2M Beca, pers. com.).
Ambient environment	Depth of sea at discharge location (m)	8.4 (MLWS), 9.5 (MSL), 10.7 (MHWS)	Chart NZ6324 (LINZ, 2009) and Almanac (LINZ, 2013)
	Wind speed (m/s)	2	Recommended conservative value (Doneker and Jirka 2012) – as calmer conditions produce the lowest initial dilution.
	Darcy-Weisbach friction factor *f*	0.025	Typical values for coastal areas range from 0.020–0.030 (Doneker and Jirka 2012).
	Velocity of the ambient water (ocean) (m/s)	0–0.15 in increments of 0.01	Current velocities at diffuser site from the 1-year Delft2d simulation range up to 0.15 m/s
	Density of the ambient water (kg/m^3)	winter = 1026.56 summer = 1024.86	Based on winter and summer sea temperatures of 7.5°C and 16.5°C (Greig et al. 1988); and a salinity of 34 psu (based on Heuff et al. 2005).
	Diffuser length (m)	12	Assuming 6 m between risers
Diffuser	Distance from nearest shoreline to nearest effective port (m)	1599	CORMIX parameter to nearest land but does not affect results in this case as only looking at near-field
	Distance from nearest shoreline to furthest effective port (m)	1607	
	Port height above the seabed (m)	0.5	Diffuser ports 0.5 m above seabed (I. Goss, OCEL, pers. com.).
	Diffuser pipeline slope on seabed	0.002	From sounding depths in NZ6324 (LINZ, 2009)
	Port diameter – equivalent circular diameter (m)	0.021, 0.025, 0.036, 0.047, 0.053, 0.057	Calculated from discharge rate and jet velocity for an example PROCO duck-bill valve e.g., 0.021 m for discharge rate of 0.0017 m^3/s, 0.025 for discharge rate of 0.0034 m^3/s, …
	Contraction ratio	1.0	Ports duck-billed with bell-mouth entry to duck-bill flange.
	Number of effective ports	6	Based on hydraulic performance incl. Froude numbers over the range of discharges
	Alignment angle, γ (°)	140	Angle between prevailing ambient current and outfall line.
	Number of ports per riser	2	Arranged on opposite sides of riser
	Vertical angle, θ (°)	0	Ports discharge horizontally.
	Direction of ports on each side	Same	

[a] for the other ambient velocities or effluent flows, linear interpolation of simulated CORMIX initial dilutions used.

3.3 Delft3d model features

Akaroa Harbour was modelled using the Deltares Delft3d hydrodynamic modelling suite.[5] The curvi-linear, 2-dimensional or 3-dimensional (multi-layer) semi-implicit model finds numerical solutions for the Navier-Stokes equations for momentum whilst conserving mass through the principle of continuity (Deltares, 2011).

Physical processes in the model can be parameterised and simulated through specifying for example, eddy scales, turbulent-closure schemes, surface and bottom boundary conditions, surface winds and pressure fields, wave-current interaction, surface heating, salinity & temperature structure and the earth's rotational effects.

The Delft3d model can be forced at open and source input boundaries by oceanic/estuarine tides, freshwater and heat sources. These forcing mechanisms produce the essential boundary physics required to simulate barotropic (surface-pressure gradients) and baroclinic (internal pressure gradients driven by horizontal and vertical water-density gradients) in the model domain which allow variation in seawater density to be included in model solutions.

For Akaroa Harbour, a depth-averaged Delft2d model was run in barotropic mode assuming no density stratification of the water column occurs (e.g., differential warming or cooling of the surface layer or freshwater river sources), which is a reasonable assumption for the tidally-dominant Akaroa Harbour with low river input relative to the large low-water spring tide volume of the Harbour (Section 2.1). While vertical density stratification (especially from temperature gradients) does occur at times in the Harbour, as observed by Heuff et al. (2005), it is unlikely to have a major influence on effluent concentrations in shallow near-shore coastal sites. Furthermore, undertaking a comprehensive field programme over a 1-year period to obtain conductivity-temperature profiles measurements within the Harbour and along the outer sea-boundary of the model is a large and expensive undertaking for what is a second-order effect. A shorter simulation of a well-mixed model, but with multiple depth layers, showed only marginal differences with depth in current velocities in the middle Harbour. In the end, the results for virus concentration factors at the coastal sites (see Section 6) were predominantly influenced by initial dilution processes (which depend on current speed and effluent flow rate) and solar inactivation, with subsequent dispersion processes including the effect of residence times within the Harbour, only a secondary contribution to the reduction in virus concentrations.

The momentum from the actual discharge from the outfall diffuser is very small, relative to the tidal fluxes in the middle harbour, so the additional momentum imparted to the flow by the discharge was not included in the hydrodynamic model. The open offshore boundary for the Akaroa Harbour model was forced with tide heights from the NIWA EEZ tidal model (Section 2.3).

3.4 Far-field modelling overview

The Delft2d model was run using ocean tides extracted from the NIWA EEZ-tide model and hybrid wind boundary condition as described in Section 2.2. The model results were then compared to tide height and current velocity measurements. The model was then calibrated

[5] http://www.deltaressystems.com/hydro/product/621497/delft3d-suite

by iteratively changing calibration parameters (Section 4.1) until modelled and predicted current-velocity vectors and tide height were in best agreement.

The calibration process determines how well the model can predict tides and currents at each of the field sites under a range of conditions (see Section 4). Given a good fit between the observed and predicted values the model can be confidently used to make predictions at other sites in the Harbour.

In this investigation, we utilised the tracer module embedded within the Delft2d hydrodynamic model to simulate effluent releases of a constant load of 1 unit mass per second for the 1-year simulation over 2013 to determine the far-field physical dilution at the 14 specified sites. In a second 1-year simulation for the same conditions, the outfall discharge hydrograph in m^3/s (Figure 5-1) was explicitly modelled as a component of the effluent load with a constant effluent concentration of 1 unit mass/m^3 to determine the pro-rata effect of varying effluent discharge on reduction of concentrations at the specified sites.

However, the tracer module used assumes no decay of effluent constituents (to facilitate fast computer run-times for the 1-year simulations). Also, the depth-averaged Delft2d model is a far-field dispersion model and does not have the very high-spatial resolution required to simulate the initial dilution processes at sub-metre scales. Consequently, post-processing of the dispersion model results included the extra factors for initial dilution (from the results of the near-field CORMIX model and DIFFUSER) and microbial inactivation (EXCEL-based algorithm- Appendix 1) to form the far-field physical dilution and inactivation for viruses between the finish of the initial-dilution (near-field) phase near the outfall diffuser and reaching each of the specified coastal sites.

3.5 Delft2d model grid establishment

The curvilinear grid the Delft2d model was established from bathymetry data sourced from:

- Sub-tidal sounding data (relative to mean sea level) supplied by the University of Canterbury (Hart et al. 2009) and obtained during a project for Environment Canterbury (see Figure 3-4).
- Offshore and intertidal soundings from Land Information NZ Hydrographic Chart NZ6324 (LINZ, 2008) for Akaroa Harbour obtained in digital form from the LINZ Data Centre. These depths were relative to Chart datum established in 2008.
- Shoreline data digitised from aerial photos.

The intertidal bathymetric data from Hart et al. (2009) were adjusted to Chart Datum (subtracting 1.5 m) and combined with the LINZ (2008) subtidal data into a terrain model using the ARC GIS software programme. This data was then interpreted using Arc GIS into a 20 m raster surface of the model domain and exported as an XYZ point file for Delft3d gridding (Figure 3-5).

The curvi-linear grid generator in the Deltares modelling suite was used to generate the grid shown in Figure 3-5, with grid cells coarser at the open boundary off the coast of Banks Peninsula and reducing to around 100 m cells in the vicinity of the proposed outfall in Akaroa Harbour (French Bay).

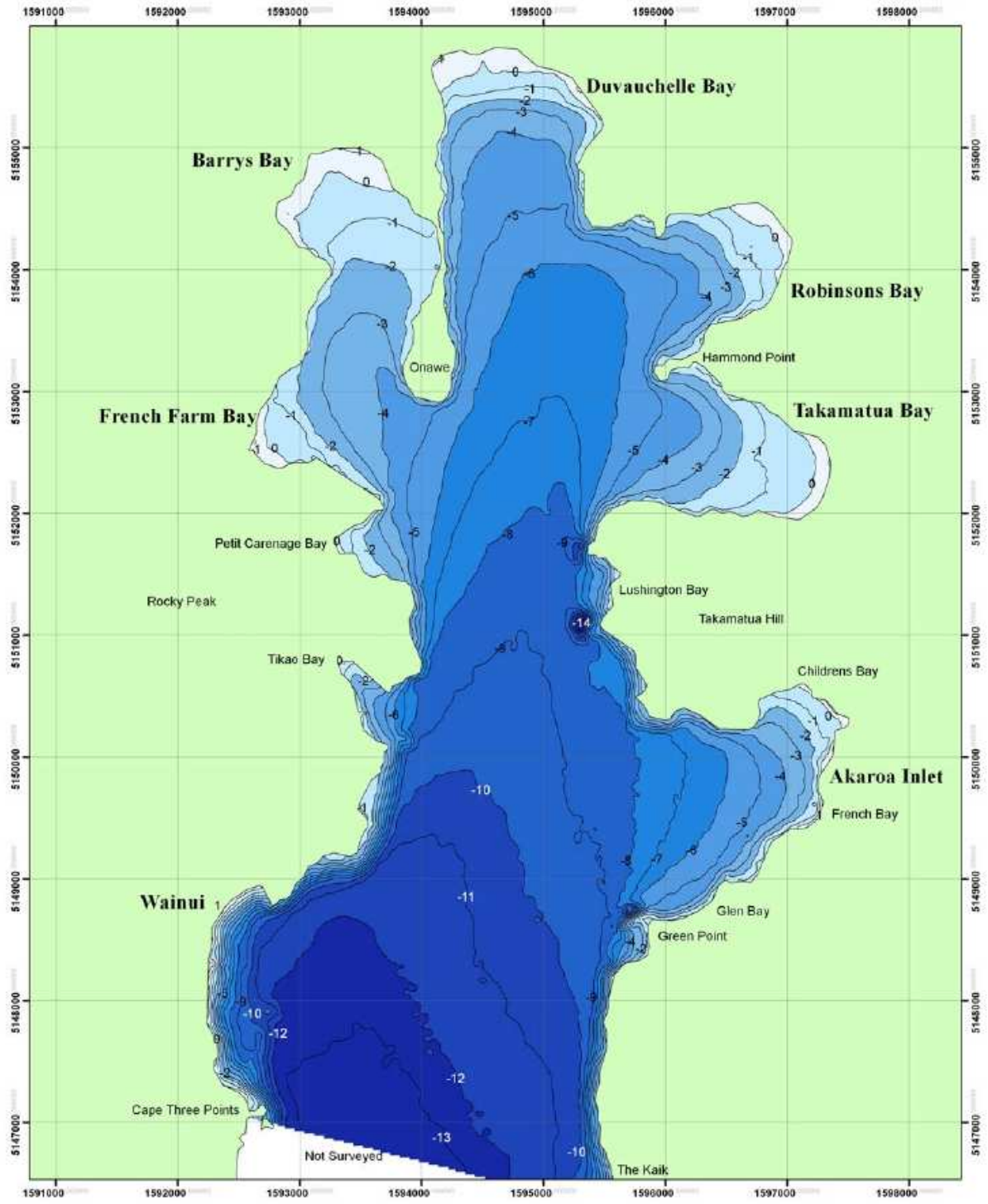

Figure 3-4: Bathymetry of upper Akaroa Harbour relative to mean sea level (MSL). Coordinate system in NZTM and MSL is approximately 1.5 m above Chart Datum. [*Source*: Map 2, Hart et al. (2009)].

The depths (to Chart Datum) processed to form the curvilinear model grid for Akaroa Harbour are shown in Figure 1-2 and Figure 3-5, with the final mesh shown on the right-hand panel of Figure 3-5.

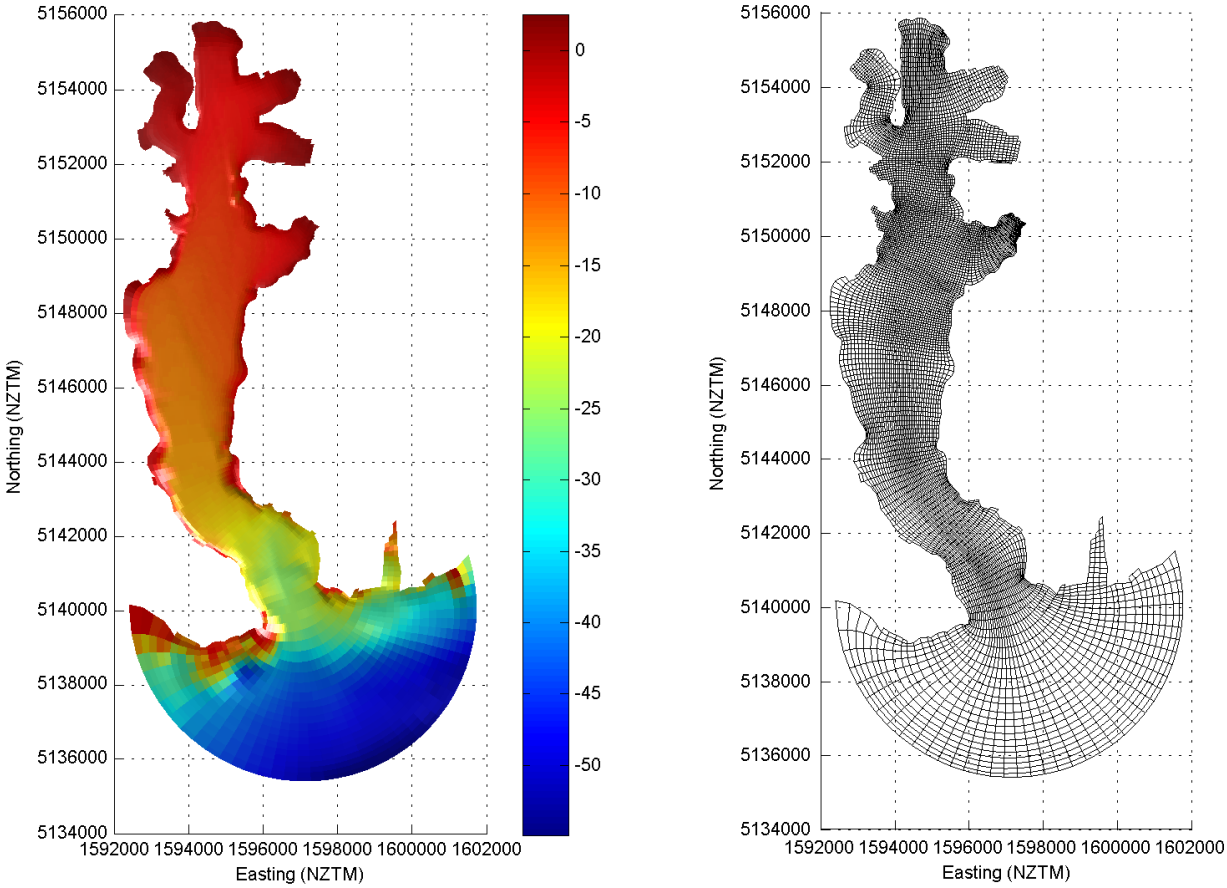

Figure 3-5: Akaroa Harbour model curvilinear mesh grid. The black squares (right) represent the mesh elements. Coloured shading (left) represents bathymetric depths (Chart Datum), negative values in key are depths below Chart Datum. Coordinates in NZ Transverse Mercator (NZTM).

3.6 Virus-inactivation algorithm

In developing a water quality model for pathogenic viruses we need to incorporate UV-inactivation processes in a rigorous manner—incorporating dark versus sunlight conditions (including shading), seasonality, vertical UV attenuation, and cloudiness.

A microbial inactivation algorithm, broadly applicable to viruses, was updated by Graham McBride (NIWA) from a previous algorithm used for QMRA studies for outfalls in Taranaki, and is described in detail in Appendix 1.

The algorithm was coded into a macro embedded within Microsoft EXCEL, which also included as input the hourly solar radiation data from the Akaroa EWS (Figure 2-5) for the 2013 calendar year.

The input parameters used in the microbial inactivation EXCEL macro are listed in Table 3-2.

Table 3-2: Parameters and values used in the microbial inactivation algorithm described in Appendix 1.

Parameter	Value	Notes
deglat	–43.8	Latitude in degrees, negative for Southern Hemisphere.
alphasr	7°	Solar altitude at sunrise (= 0 for flat unobstructed horizon) – angle calculated from mid-harbour to peak of surrounding hills to the west.
alphass	7°	Solar altitude at sunset (= 0 for flat unobstructed horizon) - angle calculated from mid-harbour to peak of surrounding hills to the east
k_d (h^{-1})	0.015 0.044	Winter and summer dark inactivation coefficient.
k_s (m^2 MJ^{-1})	0.05 0.07	Winter and summer insolation-based daytime inactivation coefficient.
k_{att} (m^{-1})	1.0	Underwater UV attenuation coefficient (see Section 2.4).
d (m)	2*	Depth below the surface considered for inactivation.

* because the experimental inactivation results used in Appendix 1 were based on 0.6 m deep containers, *d* was set to 1.4 m in the algorithm to avoid double counting, but effectively covers a 2 m depth.

The output from the EXCEL algorithm is a factor quantifying the reduction in concentration of viruses over the time step considered, which was 15-minute intervals for the 1-year simulation (e.g., a factor of 1 = no reduction). The effect of this reduction factor is minimal at night and low during winter cloudy days.

These 15-minute concentration factors for inactivation were later multiplied over the period of the relevant time-of-travel lag for the plume to reach each of the specified sites, which was determined from the delayed-response times in the Delft2d simulation for the rainstorm discharge events.

4 Calibration of the hydrodynamic model (water levels and currents)

The hydrodynamic characteristics (water levels and currents) of Akaroa Harbour were simulated by a Delft2d model set up on the grid outlined in Section 3.5.

4.1 Calibration and validation process

Calibration of the hydrodynamic model involved simulating hydrodynamic conditions over a specific time period where field measurements were available, and comparing simulated water levels, current patterns and magnitudes with the measured data. The calibration process determines how well the model can predict tides, currents, and salinities at the locations where measured data are available. The model is calibrated by iteratively changing calibration parameters until modelled and predicted vectors or scalars at the measured locations are in optimum agreement. The calibrated model is then validated by comparing further model simulations with different sets of measured data but not changing the model parameters and set-up. Given a good fit between observed and predicted values, the calibrated model can be used to make predictions at other sites in the estuary and for other time periods.

The following “tuning” parameters are adjusted in the hydrodynamic model to achieve a best fit between modelled and observed values:

- Smagorinsky eddy coefficient: Simulates horizontal shear in the model and causes change in the amplitude of surface elevations and the magnitude of current speeds.
- *k*-ε Vertical turbulence closure: Controls vertical mixing in the water column and impacts on vertical stratification in the model due to freshwater inputs.
- Bed roughness (z_0): Controls the phase (timing) and magnitude of water levels and current flows.

The measure of the ‘goodness of fit’ between observed and predicted (Appendix 2) was then estimated through the:

- Skill – A measure of the difference in the variance between the observed and predicted signal.
- Root mean square error (RMSE) – A measure of the unexplained difference between the observed and predicted signal. The root mean square (RMS) of the pairwise differences of the two data sets can serve as a measure how far on average the error is from 0.
- Bias: The residual offset between two time series. ± bias indicates a positive/negative offset in time series data. Positive bias indicates that the model is over predicting relative to the measured value.
- Cross-correlation function (R_{xy}) – A coefficient that describes the strength in the phase relationship (timing) between two oscillating signals. (0-1, with 0 being weak and 1 being strong).

A good indication of model skill is the agreement between observations and modelled results for both water levels and currents at different locations in the harbour. Data for both water level and currents were not available so to address this, tidal elevation records at Akaroa, Duvauchelle and Wainui (Figure 1-2) sites were subject to least-squares tidal analysis using the method of Pawlowicz (2002) to generate tidal water level data for times when current meter data were available. The synthesised tides were compared to the modelled sea levels, and showed that the least squares tidal harmonics fit explained 99% of the measured variance (Figure 4-1).

4.2 Tidal heights

Results for tidal height, relative to mean sea level (MSL) = zero, from a 1-month simulation for November/December 2013 are shown in Figure 4-1 for 3 locations (Akaroa Wharf, Duvauchelle Bay and Wainui Bay). There is a very good comparison with tidal harmonic predictions over the same month for these 3 sites based on tidal constituents extracted from tide-height measurements in 2008, as shown by the summary statistics in Table 4-1.

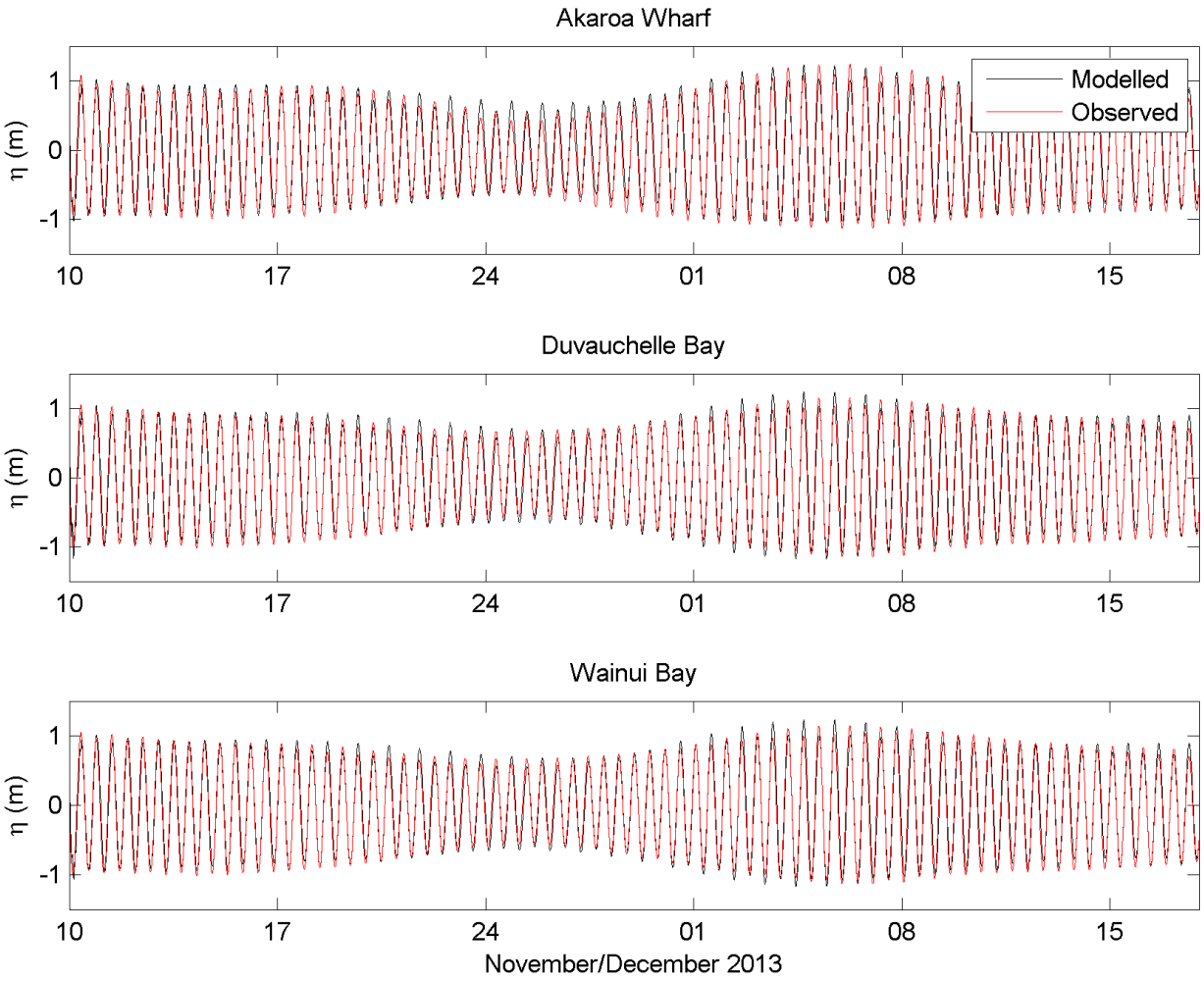

Figure 4-1: Comparison of tidal heights (relative to MSL) from the Delft2d simulation (black line) with tide predictions based on observational data (red line). Tidal predictions for the 3 locations were based on tidal constituents extracted from tidal measurements for different periods.

Table 4-1: Calibration results for water levels at Akaroa Wharf, Duvauchelle Bay and Wainui Bay represented by skill, root mean square error (RMSE), bias and cross-correlation.

Location	Skill score (%)	RMSE (m)	Bias (m)	R_{xy}
Akaroa Wharf	0.96	0.02	-0.01	0.98
Duvauchelle Bay	0.98	0.01	-0.01	0.98
Wainui Bay	0.97	0.02	-0.02	0.99

4.3 Tidal and wind driven currents

4.3.1 Calibration of currents

A 500 kHz SonTek Acoustic Doppler Profiler current meter (ADP) was deployed for this project over a period of 1 month (13 November to 18 December 2014) for the purpose of calibrating the hydrodynamic model of the Harbour at –43.807° N and 172.9368° E (see site location in Figure 2-1), which is in just over 8.0 m depth below Chart Datum. The ADP frame that sits on the seabed is shown in being lowered over the side of the vessel.

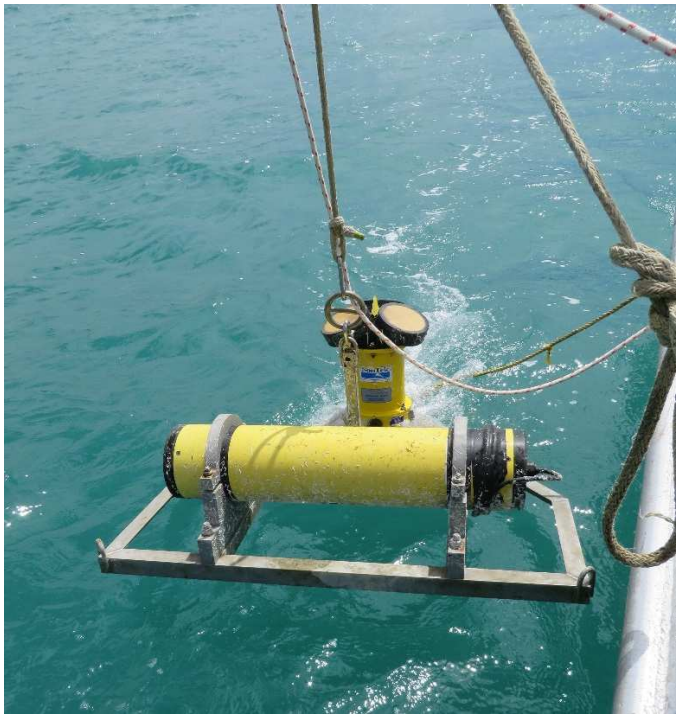

Figure 4-2: Sea-bed mooring frame comprising the 500 kHz SonTek ADP and acoustic mooring release being lowered from the NIWA vessel.

Comparison of measured current-velocity data (derived from a single point), with modelled currents (averaged over a model cell of at least 100 m scales for Akaroa), will always show up differences that are related to the spatial scale of the current-velocity field. There will also be differences resulting from physical processes not included in the model forcing e.g.,

cross-harbour seiching at short-time scales was not able to be replicated in the model without further research and generating spatially-varying winds throughout the Harbour.

To isolate the tidal component of the ADP current meter record, tidal harmonic constituents were extracted from the depth-averaged ADP record using a least-squares tidal harmonic analysis *t-tide* method by Pawlowicz (2002). The tidal *U* (east-west) and *V* (north-south) components of the ADP current-meter data is shown in Figure 4-3 (heavy lines) compared to the raw measured depth-averaged currents (thinner lines). The measured currents up and down the Harbour axis (*V*-component) at the ADP site show this component is dominated by tidal forcing. The measured east-west U-component in the ADP data is a mix of tidal forcing at 12.4 hour periods and high-frequency seiching to and fro across the Harbour at 1-1.8 hour periods with small currents of no more than 0.05 m/s. Seiching is unlikely to greatly influence plume dispersion patterns in the Harbour as they are small high-frequency to and fro motions with a negligible net residual (net) current.

Having extracted the tidal component of currents measured by the ADP current-meter, these tidal currents can be compared with the tidal component of currents predicted by the model to ensure the primary forcing is being accurately simulated. The modelled depth-averaged currents from theDelft2d model were forced by not only tidal elevations, but also ocean storm-surge heights on the offshore boundary and the hybrid wind time-series was applied equally across the model domain. Consequently, to compare only the tidal component of the modelled currents at the ADP site with the tide component from the ADP record, the modelled currents were also analysed using *t-tide* (Pawlowicz, 2002).

Figure 4-4 show the result of the direct comparison between time series of measured tidal currents (from tidal harmonics) and modelled depth-averaged *U* (East-West) and *V* (North-South) tidal-current components. Visual comparisons of the tidal component of velocity time series from the ADP record with the modelled tidal currents indicates good agreement.

The visual comparison is supported by the error analysis shown in Table 4-2 for all tidal constituents. For the current-meter site, the model skill score (with 1= perfect fit) for the tidal component of the currents was 0.98 and the bias[6] is of the order of ±0.02 m/s. The root mean-square error[7] (RMSE) for both *U* and *V* component of velocity were less than 0.06 m/s. These values are comparable to the accuracy of an ADP current meter. The cross-correlation function (between the modelled and measured tidal currents) of >0.97 indicates excellent agreement in the phasing between the observed and modelled tidal currents.

[6] Bias is defined here as the offset between the average of both time series (measured and modelled)
[7] When two data sets—one set from a model prediction and the other from actual measurements of a variable —are compared, the root mean square (RMS) of the pairwise differences of the two data sets can serve as a measure how far on average the error is from 0. Especially useful when variates show positive and negative sinusoid behaviour like tides.

Table 4-2: Model calibration results for comparing synthesised tide-only current components of velocities between the modelled and measured currents in Akaroa Harbour. RMSE = root mean square error, bias is difference between average of both datasets, and R_{xy} is the cross-correlation, which describes the strength in the phase relationship (timing) between two oscillating signals (0 being weak and 1 being strong).

Location	Velocity component (m/s)	RMSE (m/s)	Skill score (%)	Bias (m/s)	R_{xy}
Akaroa Harbour ADP current-meter site	East-west (*U*)	0.06	0.98	0.01	0.97
	North-south (*V*)	0.05		-0.02	0.98

Assessment of the hydrodynamic model skill and accuracy for the total modelled current – both tides and non-tidal components – was undertaken by comparing the model results with the low-pass filtered ADP data, which excludes the higher-frequency seiching that was not explicitly simulated in the hydrodynamic model.

Figure 4-5 shows the result of the direct comparison between time series of low-pass filtered ADP currents and the modelled depth-averaged *U* (East-West) and *V* (North-South) current velocities. Table 4-3 lists the model calibration statistics for the comparison.

The plot and statistics show the hydrodynamic model is performing well on the timing of the currents and the root mean-square error, but with somewhat less skill in matching the overall current-velocity time series including peaks, than for the tide-only comparison (Table 4-2). This is expected, as wind fields in particular are very complex within the drowned valley that forms Akaroa harbour, the possible presence of continental shelf wind-induced currents influencing flux into the Harbour from offshore, and subtle differences that ensue from stratification of the water column in the Harbour at various times when conditions are conducive to vertical-density gradients forming.

Overall, the hydrodynamic model is performing sufficiently to include most of the tide and wind-driven variability in the measured current-meter data, given model-grid cell average predictions (e.g., 100×100 m scale) tend to produce smoother results than a single-point measurement that samples all possible hydrodynamic processes at work. Also, the aim of producing a 1-year simulation covering a wide range of environmental conditions (tide, wind and seasonal solar radiation) was to develop a cumulative frequency distribution of virus concentration-reduction factors that is not necessarily reliant on achieving an exact match of predicted currents through time. One aspect of this is a slight under-prediction of current velocities by the model (e.g., Figure 4-5), which is more conservative for the initial dilution process (as slower currents lead to lower dilutions). Initial dilution is a much more dominant contributor to the overall reduction in concentrations at each of the specified sites than subsequent dispersion and Harbour mixing (Section 6).

Table 4-3: Model calibration results for comparing synthesised total current components of velocities between the modelled and low-pass filtered measured current.

Location	Velocity component (m/s)	RMSE (m/s)	Skill score (%)	Bias (m/s)	R_{xy}
Akaroa Harbour ADP current-meter site	East-west (*U*)	0.05	0.83	0.001	0.79
	North-south (*V*)	0.06		-0.024	0.85

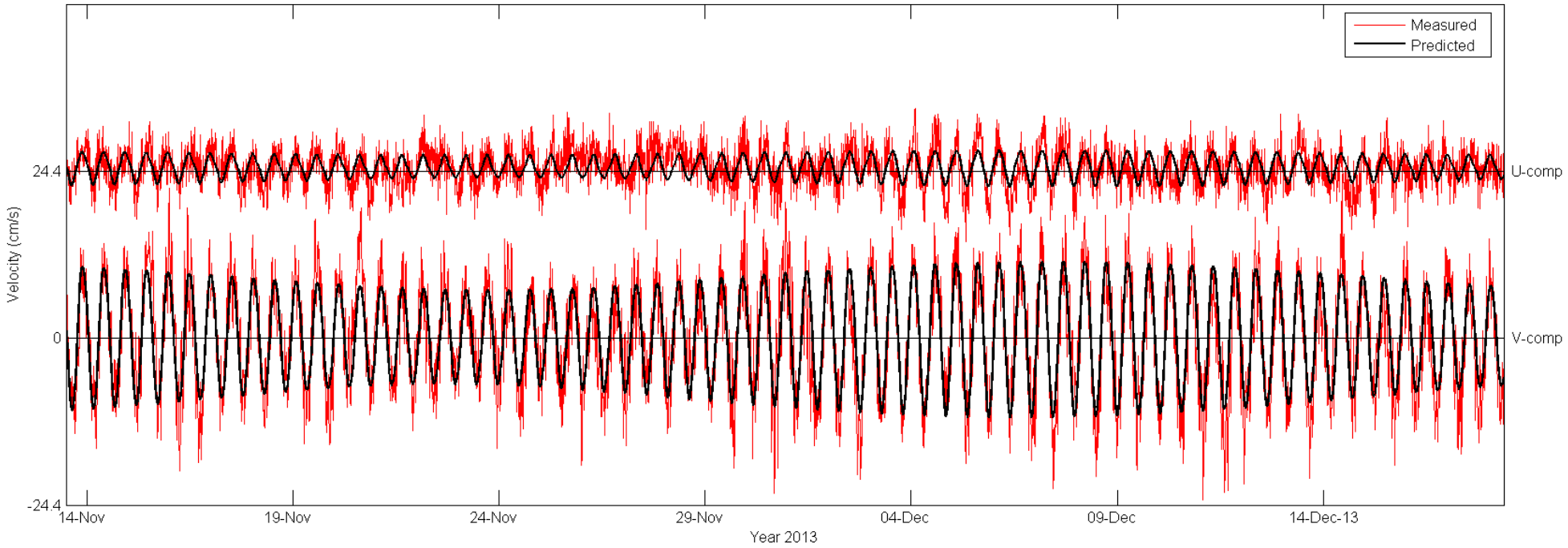

Figure 4-3: Raw depth averaged ADP velocities (red) and tidal current velocities extracted from the ADP record using t-tide (black). Tides account for 79% of the variability in the measured current velocities. Note: the higher-frequency component in the east-west U component (top) are due to seiching waves across the harbour axis.

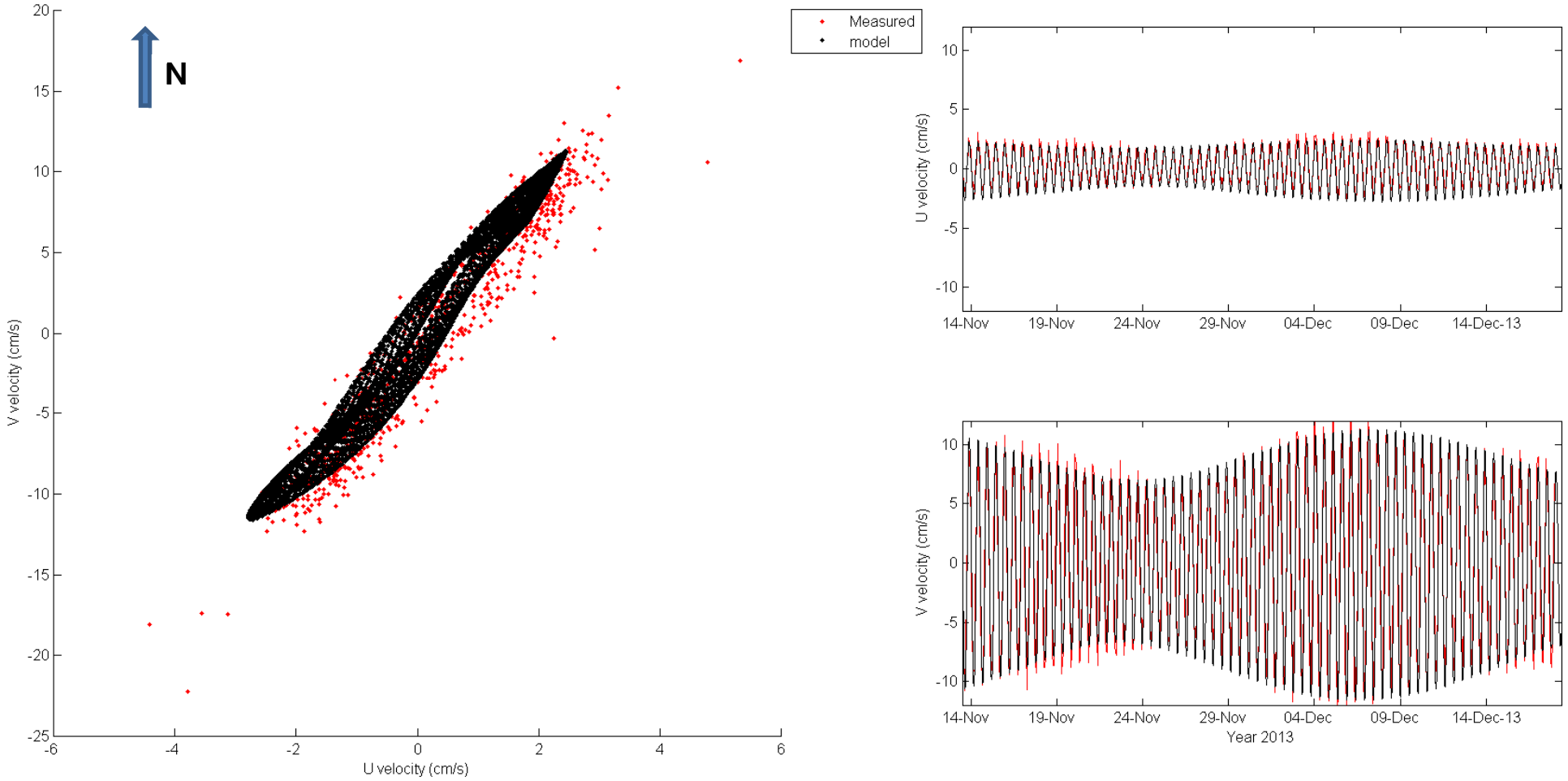

Figure 4-4: Extracted tidal *U* and *V* velocities from the ADP measurements using *t-tide* (red) vs modelled U and V tidal velocities (black).

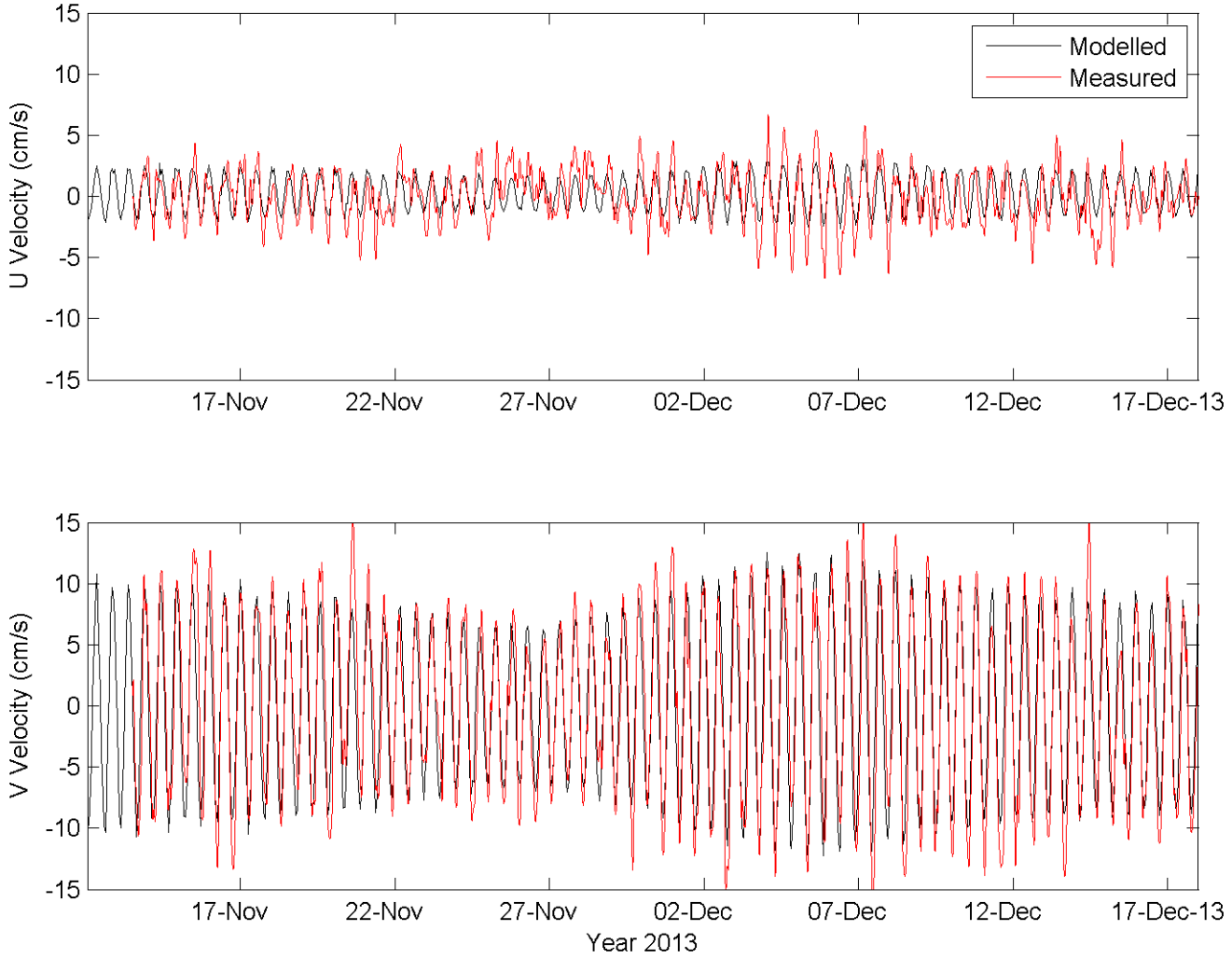

Figure 4-5: Depth-averaged modelled current-velocity components (black) and low-pass filtered current velocities extracted from the ADP record (red).

4.3.2 Harbour circulation patterns

Simulated currents for Akaroa Harbour are dominated by tidal currents, with wind effects secondary. Figure 4-6 shows the current vector maps for the harbour for the peak ebb and flood tides. The characteristic pattern for Akaroa Harbour is one of south-north flow of the tidal flow up and down the main Harbour with influx or drainage on the flood and ebb tides respectively for the side arms or embayment's.

There is a stronger ebb-tide flow around Green Point (marked on Figure 4-6) where the existing short outfall is located south of the township. This is confirmed by the previous measurements of Hicks and Marra (1988).

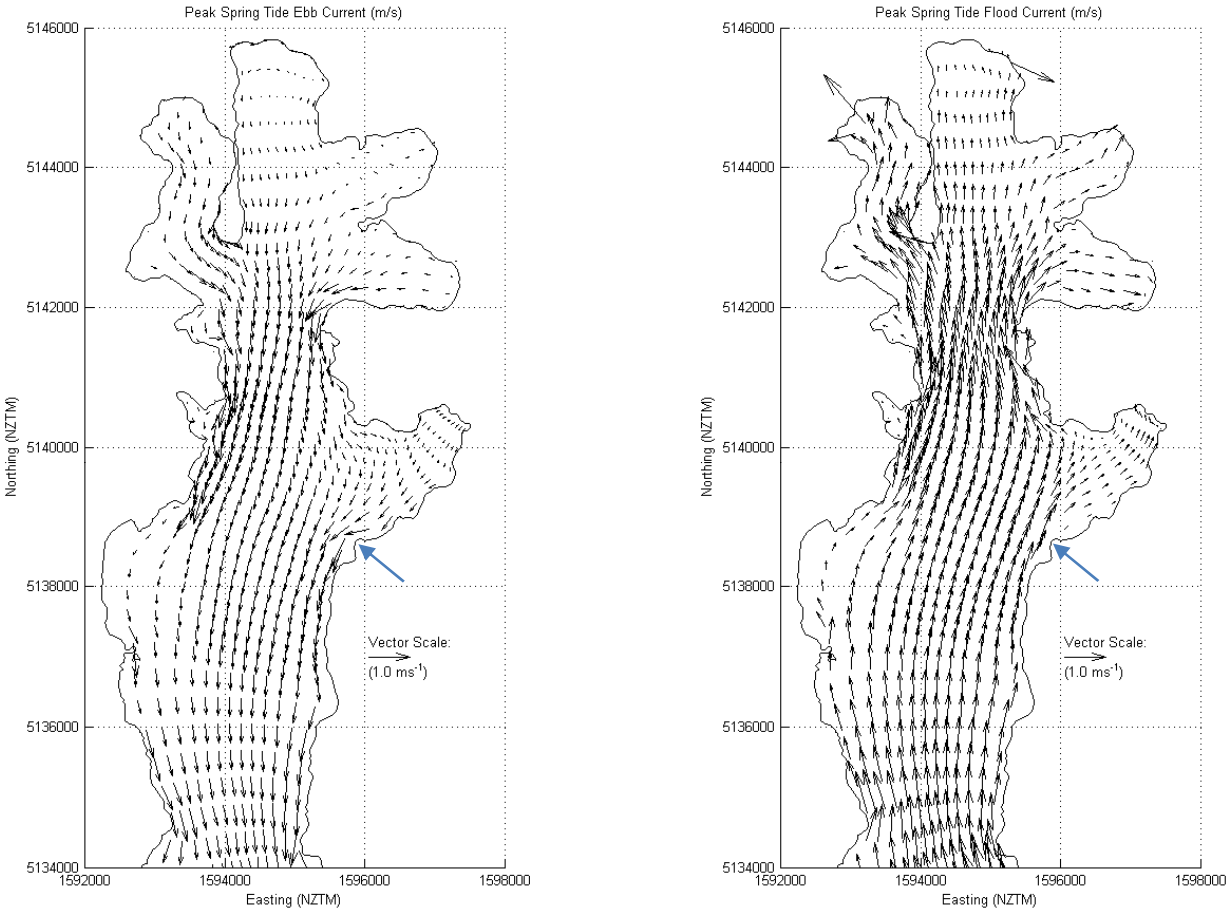

Figure 4-6: Peak ebb and flood tide current patterns for a spring tide from Delft2d simulation. Green Point is identified with a blue arrow.

Other features of the tidal-current patterns are: i) the slightly higher currents on the flood tide (versus the ebb tide) on the eastern side of the narrower section in the middle Harbour balanced by a more pronounced ebb-tide currents on the western side in Figure 4-6, and ii) . French Bay has a slight bias towards higher flood-tide currents compared to the ebb tide with the ebb-tide flow only dominating along the southern periphery past the main wharf and Green Point (Figure 4-6).

4.3.3 Current velocities at proposed outfall diffuser site

The current-velocity time series from the 1-year Delft2d simulation was extracted from the model grid cell in which the diffuser is located, for the purpose of computing the initial dilution in association with the CORMIX simulations.

Figure 4-7 and Figure 4-8 show that predicted current speeds are modest at outfall diffuser site up to 0.15 m/s with a median of 0.06 m/s. The ADP current meter showed that currents in the area can be higher than these values predicted by the model, but in terms of initial dilution, slower currents are more conservative in terms of the dilution they can achieve (with the lowest dilutions in still-water). The main driver is tidal forcing, primarily due to the monthly perigean/apogee cycle, with wind effects being secondary.

The principal direction for flood-tide set is approx. 20° True North and ebb set is ~196° True North. The 6 duck-bill valve ports (2 opposites per riser on 3 risers) will need to be approximately aligned with these principal flow directions.

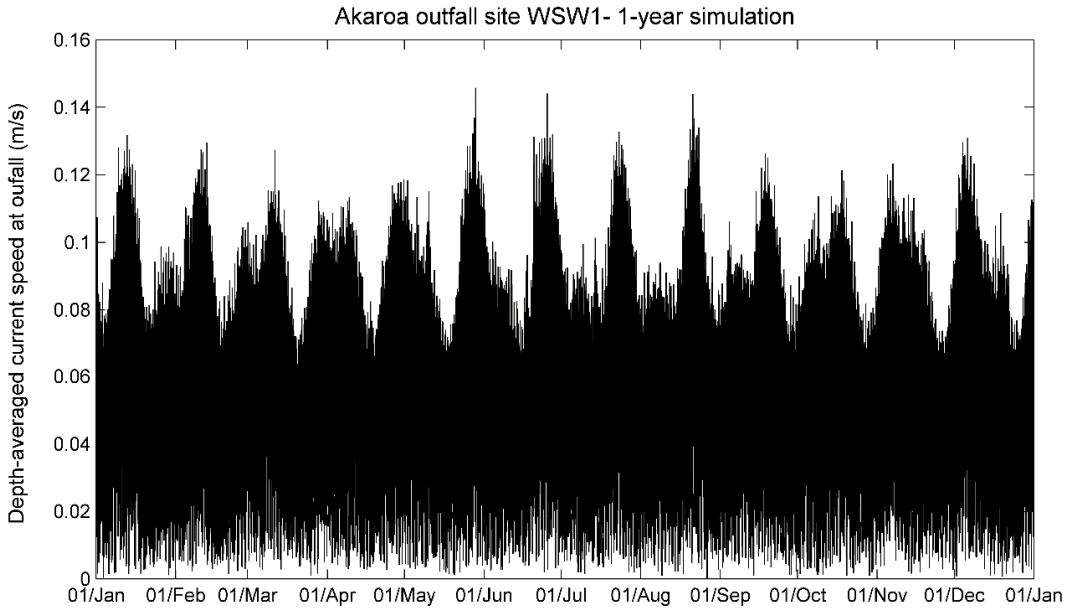

Figure 4-7: Time series of current speeds from the depth-averaged Delft2d model at the proposed outfall diffuser site for a 1-year simulation. Time series was at 15-minute intervals and extracted at the WSW1 diffuser site (2.5 km outfall).

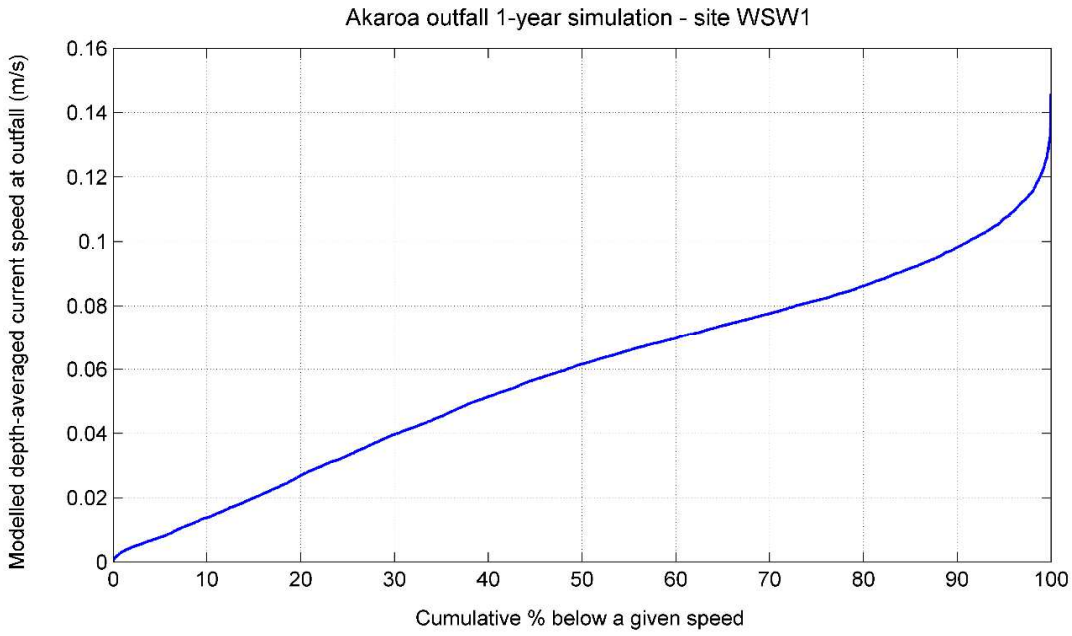

Figure 4-8: Cumulative distribution of current speeds from the depth-averaged Delft2d model at the proposed outfall diffuser site for a 1-year simulation. Time series was at 15-minute intervals and extracted at the WSW1 diffuser site (2.5 km outfall).

5 Dispersion modelling and calculation of dilutions

Dispersion and mixing of a discharge within a receiving water body occurs over a wide range of spatial and time scales, which poses a challenge in modelling the breadth of scales involved. Generally, simulation of dispersion and mixing is treated as two distinct phases:

- Near-field phase – where the buoyancy (from the freshwater effluent), momentum of the jets from the diffuser and the current speed across the diffuser govern the mixing processes. This phase occurs over a matter of several minutes and for the proposed Akaroa outfall, extends only 50-100 m, with most of the mixing complete by around 50 m from the diffuser. Because of the short time and spatial scales involved as well as 3-D mixing and buoyancy processes, the near-field phase is difficult to incorporate within a wider Harbour model, so is simulated separately with an appropriate near-field plume mixing model (e.g., CORMIX).
- Far-field phase – beyond the 50 m zone of initial dilution, the far-field mixing and dilution processes that disperse the plume (at length scales of 100's of metres to a few kilometres) are dominated by environmental conditions (e.g., tides, winds). In a semi-enclosed harbour like Akaroa, basin-wide mixing and flushing process at longer spatial and time scales (weeks to months) will also affect the overall far-field physical dilution that can be achieved and is intricately connected with the time-rate of decay for discharged substances or inactivation of viruses. At one end of the spectrum, the subsequent concentrations of a fast-decaying substance will not be influenced by the basin-wide flushing processes, but concentrations of a non-decaying substance will be largely controlled by the flushing rate (or residence time) for the harbour, rather than subsequent dispersion of the plume.

Ultimately, the near-field and far-field simulations are geared towards determining the total dilution and inactivation (S_{tot}) at each of the 14 specified sites. This will be the product of initial dilution (S_o), far-field dilution from subsequent dispersion and harbour-wide flushing (S_f) and finally the decay rate, which for viruses is mainly due to microbial inactivation from exposure to solar radiation (S_{mi}) as shown in Equation 1:

$$\boldsymbol{S_{tot} = S_o \times S_f \times S_{mi}} \qquad (\mathbf{1})$$

Subsequent dispersion and harbour mixing during the far-field phase of the discharge from the proposed Akaroa Harbour WWTP outfall were undertaken using two different modes in the Delft2d model to generate the far-field dilution (S_f) contribution to the total dilution and inactivation at each of the specified sites.

Results from the CORMIX near-field model for the initial dilution (S_o) and the algorithm for calculating microbial inactivation (S_{mi}) were then factored together (Equation 1) in a post-processing step to combine with the results from the tracer-dispersion module in Delft2d, to form a 1-year time series of total dilution and microbial inactivation for each of the 14 specified sites at 15-minute intervals.

5.1 1-year far-field tracer dispersion simulations

Two 1-year simulations from 1 January 2013 to 1 January 2014 were set up in Delft2d, by assembling the open-sea tidal height time series with storm surge and a hybrid wind time series from Akaroa EWS and the EcoConnect 12 km forecast re-analysis as input drivers for the hydrodynamic model covering the whole year.

The first 1-year simulation used a constant load of 1 mass unit per second as the input rate for the tracer (which is equivalent to a constant concentration of 1 mass unit/m^3 discharged at 1 m^3/s) for a non-decaying substance. The second 1-year simulation used a varying load, normalising the discharge concentration to a constant 1 mass unit/m^3 (and hence scalable later with known effluent concentrations) but varying the outfall discharge time series likely from the proposed WWTP by 2041. This discharge time series included the 24-hour diurnal flow and seasonal changes in effluent discharge scaled from the current WWTP measurements. Also six rainstorm events of varying peaks and durations from WWTP discharge data recorded during the 4-year period 2010–13, were incorporated into the 1-year time series for 2013, fitting the events in when similar tide and wind conditions occurred for the month of the year for the event (Figure 5-1). Other than the placement of the rainstorm events within the 2013 simulation period, the discharge time series was as supplied by CH2M Beca.

The inclusion of variable discharge rates including rainstorm events over the 1-year simulation, as distinct from separate individual simulations of rainstorm events, ultimately transfers the variability that might be expected on an annual basis (including occasional rainfall events) to the cumulative distribution of virus concentrations at specified sites used as an input to the virus risk assessment (McBride, 2014).

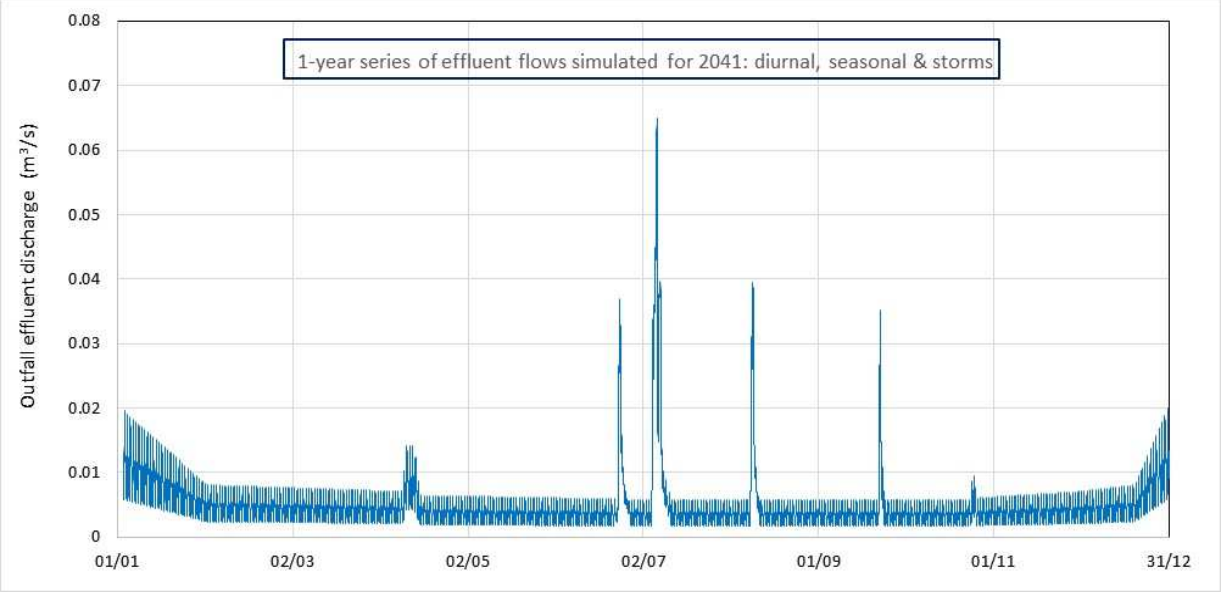

Figure 5-1: Synthesised Akaroa WWTP discharge projected for 2041 but applied to 2013 tide and wind conditions. Date in dd/mm format. Series includes diurnal flow variability, seasonal increases in the summer and 6 rainstorm events in autumn, winter and spring, when such rainstorms are more likely to occur. [*Source*: flow rate data for 2041 at hourly intervals supplied by CH2M Beca.]

Concentrations over the 1-year Delft2d tracer simulations for a “constant load” and the “varying load” (that incorporates variable discharge rates) were recorded at the sites specified in Figure 5-2. Concentrations for the varying effluent load were later divided by the “constant-load” simulation results to obtain a concentration-reduction factor that incorporates the full likely range of effluent discharge rates (including rainstorm events), which can then be inverted to calculate the far-field dilution (S_f) comprising subsequent dispersion and harbour-wide mixing and flushing for a non-decaying substance, before the microbial inactivation is factored in.

5.2 Delft2d tracer module

Delft2d has a tracer module, where a discharge of a non-decaying substance in mass units/sec can be released into the cell where the diffuser is located. Ideally, combining both physical dispersion and inactivation together for a far-field simulation would have been preferable, but computer run times would have been excessive. Using the tracer dispersion module meant a 1-year simulation was feasible in terms of computer run-time, whereas using the more sophisticated Delft2d DELWAQ water-quality dispersion module with a decaying substance (e.g., microbial inactivation) would have meant considerably longer run times to accomplish a similar dispersion simulation. Note: dis-aggregating the physical mixing processes for a non-decaying substance and later factoring in microbial inactivation for viruses during post-processing (Equation 1) is likely to be conservative by underestimating physical far-field dilutions at each site, particularly sites closer at hand to the outfall in the middle Harbour, as explained below.

Horizontal and vertical dispersion coefficients, derived for the Wellington (Lyall Bay) outfall plume investigations (Bell et al. 1992) based on dye tracing and drogue-tracking surveys, were used as mixing coefficients in the Akaroa Harbour Delft2d tracer module.

The Delft2d hydrodynamic model (e.g., current velocities) runs in parallel to the same Delft2d tracer model. The two coupled models simulate the advection and dispersion of the discharged wastewater plume around the model domain and the basin-wide mixing and flushing characteristics of the harbour (where ultimately concentrations will be in balance with the tidal exchange at the Harbour entrance with the marine waters of the Canterbury Bight).

The far-field physical dilution (S_f) was determined in post-processing as the concentration in the proximal model cell containing the diffuser divided by the lagged concentration that applies to each of the specified sites in Figure 5-2 (allowing for the average travel-time for the plume to that site). Normalising the results for each of the specified sites in this way to the concentration averaged over the 100-m model cell where the discharge was injected, rather than the effluent concentration, ensures there is minimal inclusion of any near-field initial dilution from the Delft2d results, which instead was simulated separately by the more appropriate near-field CORMIX model. Finally, the concentrations from the “varying load” simulation, which incorporates the varying discharge rate, relative to the concentrations at each site from the “constant load” simulation where factored into the far-field dilution (S_f).

The plume travel-time lags for each of the 14 specified sites (Figure 5-2) were determined by averaging the lag times between the initial rise in effluent discharge from the diffuser during the higher-discharge rainstorm events (Figure 5-1) and the onset of a corresponding rise in concentration at each site. The summary of calculated plume travel-time lags for each

specified site are listed in Table 5-1, listed with the same site codes used in the QMRA report (McBride, 2014).

Figure 5-2: Specified sites for which total dilution plus inactivation and concentration-reduction factors were determined. White line is proposed 2.5 km outfall alignment and yellow line near site 7 is the existing outfall.

The Delft2d tracer-module simulation shows quite long plume travel times to reach the selected coastal sites (Table 5-1), with sites in the upper Harbour (12-FFB and 13-TaB) having lag times of over 8 days, which will allow substantial microbial inactivation or decay for other substances to occur.

Table 5-1: Representative plume travel-time lags for each of the specified sites in Akaroa Harbour shown in Figure 5-2.

Site	Name	Site code	Lag (hrs)	Lag (days)
1	Lushington Bay	LuB	76.25	3.18
2	Childrens Bay	ChB	65.25	2.72
3	Offshore Childrens Bay	OCB	59.75	2.49
4	French Bay -CBD	FBC	61.0	2.54
5	French Bay -Wharf	FBW	63.0	2.63
6	Glen Bay	GnB	66.75	2.78
7	Existing outfall/WWTP	ExW	15.0	0.63
8	The Kaik	ThK	46.25	1.93
9	Ohinepaka Bay	OhB	57.75	2.41
10	Wainui	Wai	70.25	2.93
11	Petit Carenage Bay	PCB	125.75	5.24
12	French Farm Bay	FFB	208.0	8.67
13	Takamatua Bay	TaB	193.75	8.07
14	Middle Harbour (160 m N outfall)	MHb	7.0*	0.29

* This is a representative (average) lag time from the model covering simulated high discharge peaks coinciding with different times during a tidal cycle – on a flood-tide the lag will be shorter and longer on the ebb tide.

Using a constant discharge source of a non-decaying substance in the Delft2d tracer module within a semi-enclosed harbour will also incorporate the basin mixing and flushing processes at larger spatial and timescales. Consequently, for the Akaroa Harbour simulations of a non-decaying substance (starting with a background concentration of zero), a transition period of up to 4 months shows up in the model results until the Harbour background concentrations reach a dynamic equilibrium between the discharge load and tidal exchange through the Harbour entrance (both can vary). Given we require far-field dilutions when the subsequent dispersion and basin-wide flushing processes are operating in the long term, the modelled start-up transition in concentrations at each of the specified sites was low-pass filtered to detrend the initial transitory section and line-up with the rest of the concentration time-series to ensure the 1-year simulation results only apply to dynamic–equilibrium conditions.

Once the Harbour reaches an equilibrium background concentration level, the far-field dilution S_f of the conservative tracer (including the effect of the basin-wide residence time and tidal exchange of the Harbour) is only an average of around 2-fold at most of the sites, excluding any decay or microbial inactivation for viruses, which will be factored in later. What this is illustrating is the subsequent dilution of the plume, at short to intermediate time and spatial scales, as it is diluted and travels to the specified site, is over-run by the more dominant longer-timescale effect of the harbour flushing characteristics via tidal exchange at the Harbour entrance (when modelled using a conservative tracer). All of these physical far-field processes are simulated together by the Delft2d model. This is a feature of semi-enclosed harbour basins that is not present in open coastal or ocean waters, where plume dispersal dominates far-field dilution (for both conservative and/or decaying tracers).

Introducing the effect of microbial inactivation for viruses will substantially increase the combined far-field reduction in concentrations at the specified sites, leaving physical far-field dilution as only a minor contributor to total dilution and inactivation.

The disaggregation of time-related decay or inactivation processes from the far-field dilutions for a non-decaying substance that apply in a harbour such as Akaroa is conservative, as

plume dispersion and dilution in the model is partially governed by concentration gradients (differences) between the plume and the background concentrations of the receiving waters – but nevertheless the harbour flushing characteristics are still present even for slowly-decaying substances or viruses in this case. Therefore the approach adopted is likely to have somewhat underestimated far-field physical dilutions at each site (which is more conservative), particularly for sites closer at hand to the outfall in the middle Harbour.

5.2.1 Akaroa Harbour residence time

As an aside, the simulation of a constant discharge source of a non-decaying substance in the tracer module is a way for determining the overall residence time for flushing from Akaroa Harbour.

The average residence time of a discharged substance into a harbour is a function of:

a) tidal volume exchanged each tidal cycle with Canterbury Bight waters

b) the large residual volume of Akaroa Harbour remaining at low tide, and

c) the catchment freshwater run-off volume relative to the overall Harbour volume, which is a very low ratio for Akaroa Harbour.

As discussed in Section 2-1, Heath (1976) calculated the residence time for Akaroa Harbour using two different analytical methods: i) assuming complete tidal mixing and exchange each spring tide; and ii) assuming mixing and exchange is limited to replacement of freshwater run-off volume with the Harbour volume (no tidal influence). Neither of the estimates provides a realistic residence time for the Harbour, because of the large residual volume of the Harbour remaining at low tide and the small mean-annual freshwater runoff to the Harbour. A much improved estimate can now be achieved using the hydrodynamic model simulation of a non-decaying substance.

The transitory period to reach a dynamic-equilibrium background harbour concentration in the Delft2d tracer-module simulations was up to around 120 days, for a discharge of a non-decaying load of 1 kg/sec starting from a zero background concentration. This is a more reliable measure of the residence or flushing time for the Harbour excluding any decay or microbial inactivation.

5.3 Short-term DELWAQ simulations

For the purposes of providing a more realistic spatial picture of the plume characteristics incorporating both physical far-field dilution and microbial inactivation, the more complex Delft2d DELWAQ dispersion model was set-up to simulate short periods based on using *E. coli* faecal indicator bacteria, which was in the module library for effluent constituents. (Note: it would take some time to develop a plug-in for virus inactivation similar to Appendix 1). The DELWAQ simulation assimilated the same solar radiation measurements from the Akaroa EWS (Figure 2-5). The simulations covered a few weeks in a January and April period of the 1-year discharge series (Figure 5-1).

The main purpose of this DELWAQ application was to provide realistic graphics to demonstrate the plume pathways and extent where inactivation was explicitly included, which is not present in the Delft2d tracer-dispersion module results for a non-decaying substance.

Some snapshots of the plume extent and approximate concentrations in terms of % effluent concentration (which excludes a component of initial-dilution in the near-field) for different tidal conditions are shown in Figure 5-3 for summer (January) and Figure 5-4 for autumn (April). These snapshots of the plume show the predominant pathway taken by the effluent plume from the proposed outfall diffuser and illustrate the effects of day-time and night-time inactivation (the plume spread being larger at night for a given upper-threshold concentration). The concentrations in the centre of the plume for autumn (Figure 5-4) are lower than in summer (illustrating the influence of lower effluent discharge rates outside the peak summer period), but is offset by a wider distribution of low concentrations due to slower inactivation in autumn (and even slower in winter).

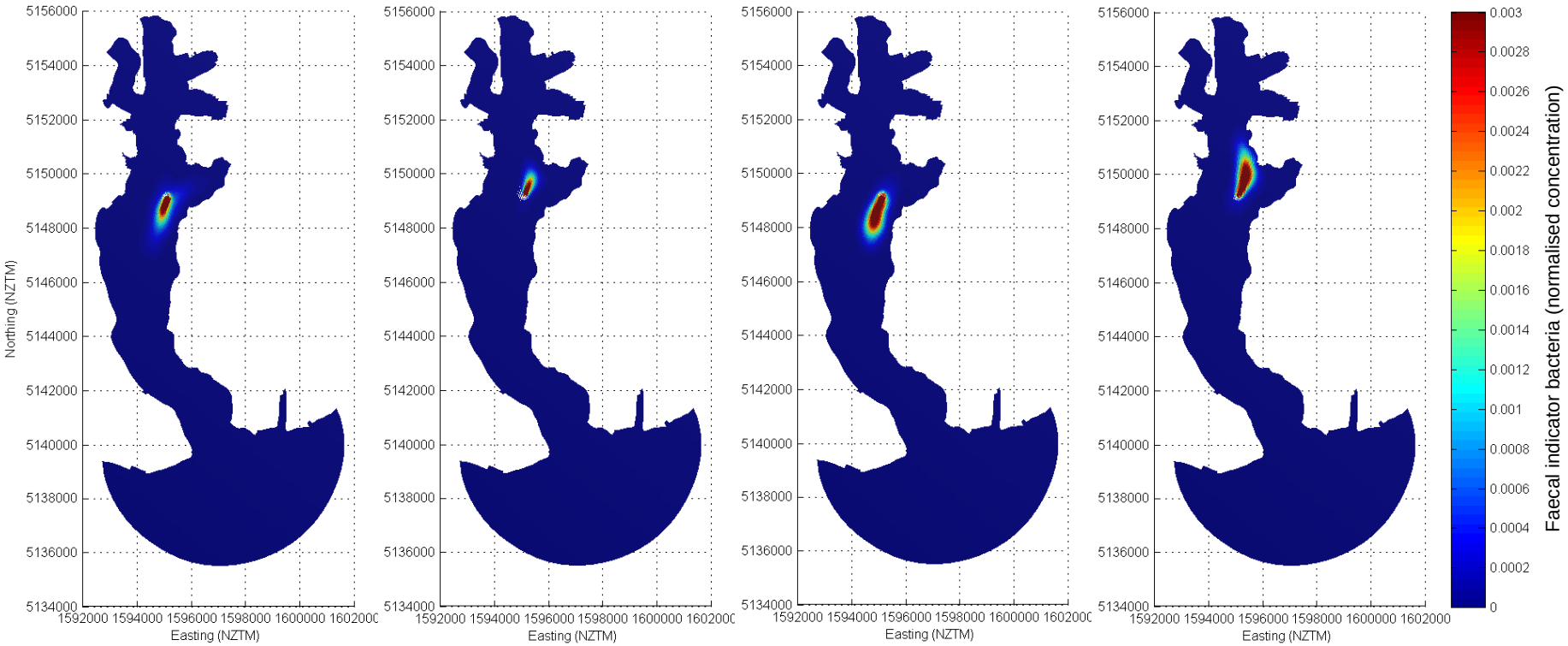

Figure 5-3: Snapshots of the effluent plume in summer (January) based on inactivation and subsequent dilution of faecal indicator bacteria using Delft2d DELWAQ module. Left to right: ebb-tide (daytime); flood tide (daytime); ebb tide (night-time); flood-tide (night-time).

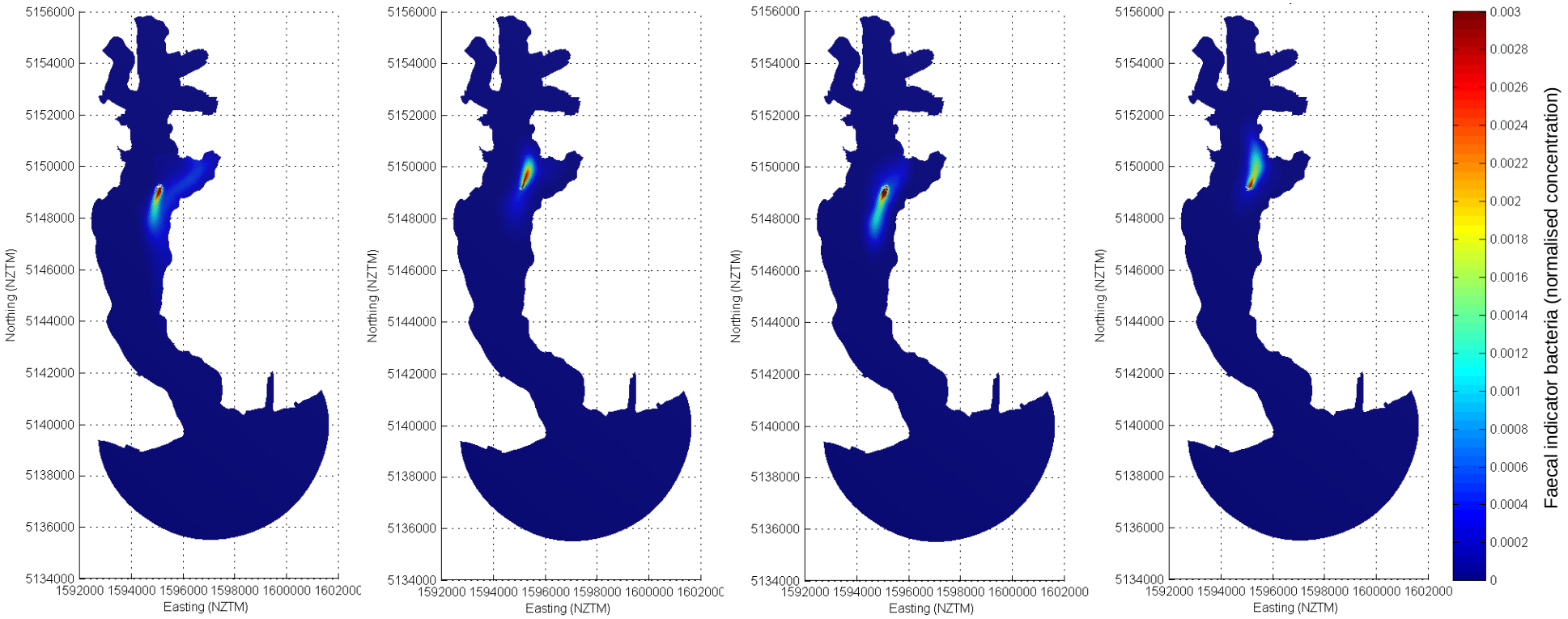

Figure 5-4: Snapshots of the effluent plume in autumn (April) based on inactivation and subsequent dilution of faecal indicator bacteria using Delft2d DELWAQ module. Left to right: ebb-tide (daytime); flood tide (daytime); ebb tide (night-time); flood-tide (night-time).

5.4 Approach adopted for a cumulative distribution of virus concentrations at coastal sites

The main aim of the 1-year model simulations was to develop a probabilistic distribution of combined subsequent dilution (from Delft2d model) and microbial inactivation factors, then factor in the initial dilution results from the CORMIX simulations, which when combined are applicable to the likely reductions in concentrations of viruses at the 14 specified sites of interest.

The Delft2d tracer simulation output results at 15-minute intervals, which sufficiently resolves the twice-daily tidal cycles and solar diurnal cycle without being unwieldy in the amount of data involved (approximately 35,000 values over 1 year). The model simulation also covers an entire year capturing varying winds, tide type and seasonal solar radiation conditions.

Post-processing the Delft2d results in Microsoft EXCEL involved:

1. applying the plume time-of-travel lags (Table 5-1) to the concentration time series for the relevant site
2. computing the time series of far-field dilution (dividing the concentrations in the outfall model by the lagged concentration time series for each site) and then
3. applying the factor related to the effluent discharge (a ratio of the results from the varying–load versus the constant-load 1-year simulation)
4. computing the final far-field physical dilutions for all 14 specified sites.

Microbial inactivation for viruses was calculated in a second EXCEL spreadsheet at 15-minute intervals using the algorithm described in Appendix 1, interpolating the hourly solar radiation data for 2013 from the Akaroa EWS (Figure 2-5).

For the near-field phase, plume-averaged initial dilutions were then determined in a third EXCEL spreadsheet by inputting 15-minute time series of the effluent discharge (Figure 5-1) and the tide level and current speed from the Delft2d modelled outfall discharge location, and applying a three-way interpolation (or look-up function) on the multiple CORMIX scenario simulation results covering the range of input parameters in Table 3-1. The DIFFUSER algorithm was used to determine the lower-bound initial dilutions for still-water conditions for the EXCEL look-up tables (as CORMIX works with a minimum non-zero threshold for current speed across the diffuser).

All three “dilution” processes: i) initial dilution S_o; ii) far-field physical dilution S_f; and iii) microbial inactivation S_{mi}, were then combined in a final EXCEL spreadsheet by multiplying each time series of these three factors at each of the sites of interest as per Equation 1 to derive a 15-min time series of total dilutions and inactivation of human-derived viruses (S_{tot}).

The final product from this modelling investigation for the QMRA process was to compute cumulative distribution functions of the total dilutions and inactivation of human-derived viruses at each of the specified sites and finally virus concentration-reduction factors, which is the inverse of total dilution) at each site. This was accomplished by sorting the thousands of 15-minute values into ascending order (lowest to highest) and calculating various

percentiles to describe the functional relationship of the dilution or concentration-reduction factor distributions.

For the delivery of results to the QMRA process, concentration-reduction factors for each specified site were initially normalised to a constant effluent virus concentration of 1 virus/m^3 in the “varying-load” Delft2d simulation. Given viruses in the influent to a WWTP are normally much higher than this low base level, the concentration-reduction factors for each site were multiplied by 1000, before being provided as input to the QMRA process. This is equivalent to a normalised concentration in the effluent of 1 virus/L. The enables a direct scaling of the concentration-reduction factors by whatever the relevant range of virus concentrations (in virus units/L) is for the proposed final effluent quality.

6 Modelling results

The main objective of this modelling investigation was to support the QMRA process and provide cumulative distributions of the concentration-reduction factors (CRFs) for 14 specified sites, covering a range of environmental and weather conditions experienced over a 1-year period. This was undertaken based on tide, wind and solar radiation conditions experienced over the 2013 year, but using projected effluent discharge rates for 2041.

The cumulative distributions of virus concentration-reduction factors have been passed over to Mr Graham McBride (NIWA) to provide one of the essential inputs to the QMRA process (McBride, 2014).

The following sections show a selection of the results to provide some insights on dilutions or inactivation for the near-field and far-field dispersion phases and to aid interpretation of the effects on public health.

6.1 Near-field: initial dilution

Figure 6-1 shows the cumulative distribution of initial dilutions that would be achieved by the specimen diffuser design situated at the end of the 2.5 km proposed WSW outfall alignment (Section 3.2.1). The distribution climbs steeply at the top end, with initial dilutions reaching above 3000-fold, which mainly relate to low night-time discharges of 1.7 L/s. The lowest initial dilutions occur for higher effluent discharges during slack-tide or slow-moving conditions at the diffuser.

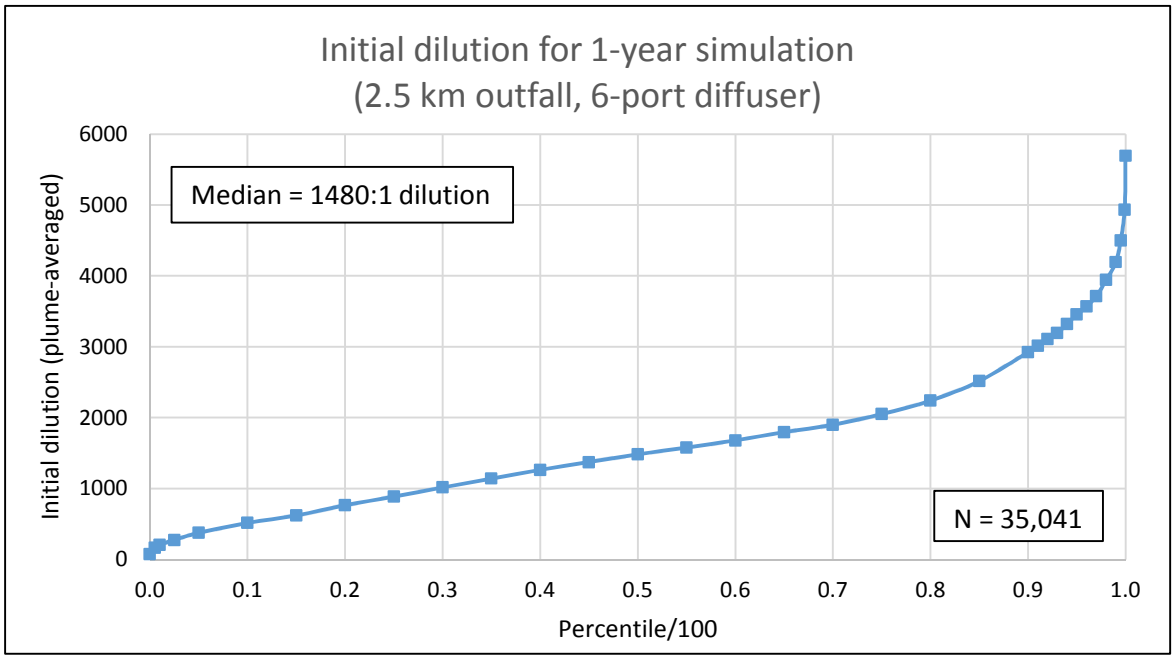

Figure 6-1: Cumulative distribution of initial dilutions computed over the 1-year simulation for the proposed outfall diffuser site (WSW1). Based on dilutions at 15-minute intervals.

Table 6-1 lists a statistical summary of the distributions of expected initial dilutions based on the 1-year simulation encompassing a variety of environmental conditions.

In most cases, the top surface of the diluted plume reached the sea surface within a few 10's of metres of the diffuser. Further initial mixing continued at the lower inter-facial surface of the plume, achieving most of the initial mixing within 50 metres of the diffuser, with some further residual initial dilution achieved in the next 50 metres. This length scale is similar to that of the model cell in Delft2d the contained the discharge location.

Table 6-1: Summary statistics for the distribution of expected initial dilutions for 2041 effluent discharge rates.

Percentile	Initial dilution
Max	5690:1
90%ile	2925:1
Mean	1590:1
Median	1480:1
10%ile	516:1
1%ile	207:1
Min	76:1

6.2 Far-field physical dilution and microbial inactivation

The main objective of the Delft2d model 1-year simulations was to:

- determine the far-field physical dilution applicable at each of the 14 specified sites during the far-field dispersion phase including the influence of harbour-wide flushing characteristics
- support the post-processing to enable a scaling function related to the outfall discharge to be applied to calculate far-field dilution factors at each site
- provide input time series for tide height and current velocity for the near-field CORMIX simulations (see previous section).

In post-processing, microbial inactivation (see Appendix 1) was applied to the far-field dilution factor to yield the total reductions in virus concentration from far-field processes at each site prior to applying the initial dilution factors (which are common to all sites).

The results for the far-field processes, as previously discussed, show that the microbial inactivation dominates over the physical subsequent-dispersion processes, which combines shorter time-scale plume dispersion processes with the influence of the residence or flushing time for the Harbour.

Inactivation, as expected is slower in winter when hourly solar radiation is lower, hence there is general decrease in the combined far-field physical dilution and inactivation. This is reflected in the median total dilution + inactivation (S_{tot}) for winter being lower compared with summer, as shown in Table 6-2.

During wet-weather events, subsequent plume dilution decreases temporarily with the increased effluent-discharge loading. These wet-weather events were embedded in the 1-year discharge time series spanning the autumn, winter and spring seasons (Figure 5-1).

6.3 Total near-field and far-field dilution and inactivation

The factors for all three "dilution" processes – initial dilution (S_o) , far-field physical dilution (S_f) and microbial inactivation (S_{mi}) – that lead to a reduction in virus concentration at the specified sites were multiplied to yield the total near-field and far-field dilution and microbial inactivation (S_{tot}). Table 6-2 shows a summary of the median total dilution and inactivation that would apply in the summer-bathing and winter[8] seasons for each of the specified sites of interest.

Table 6-2: Median total dilution and inactivation (S_{tot}) for the specified sites covering the summer bathing season and winter. Summer extends from 1 November to 31 March and winter from 1 April to 31 October.

Site No.	Site code	Summer median: total dilution + inactivation	Winter median: total dilution + inactivation
1	LuB	1.6×10^4	2.5×10^3
2	ChB	8.8×10^3	1.9×10^3
3	OCB	6.7×10^3	1.7×10^3
4	FBC	7.2×10^3	1.8×10^3
5	FBW	8.0×10^3	1.9×10^3
6	GnB	9.7×10^3	2.0×10^3
7	ExW	8.6×10^2	7.2×10^2
8	ThK	4.5×10^3	1.7×10^3
9	OhB	8.9×10^3	2.5×10^3
10	Wai	1.5×10^4	2.8×10^3
11	PCB	1.9×10^5	6.7×10^3
12	FFB	1.1×10^7	3.1×10^4
13	TaB	5.6×10^6	2.4×10^4
14	MHb	5.2×10^2	5.2×10^2

Figure 6-2 shows the full cumulative distribution (in % of the time exceeded) of the total dilution plus inactivation (S_{tot}) of viruses at each of the sites of interest. The summer-only distributions(bottom panel) show that higher total dilutions and inactivation are achieved more often when compared with the four-seasons plot (top panel), due to the more sustained microbial inactivation during the longer summer daylight hours. The lowest total dilutions plus inactivation at the upper-end percentiles for the 1-year distribution (top panel of Figure 6-2) apply to the wet-weather events that were introduced throughout the effluent discharge time series.

Site 14–MHb in the middle of the Harbour, 160 m north of the proposed diffuser site, understandably produces the lowest total dilution and inactivation. The median values for site 14 are the same for summer and winter (Table 6-2) and these occur primarily because far-field dilution and inactivation are smaller than the initial dilution closer to the outfall diffuser.

[8] Winter used in this context to cover the months from April to October (inclusive) outside the November to March summer bathing season.

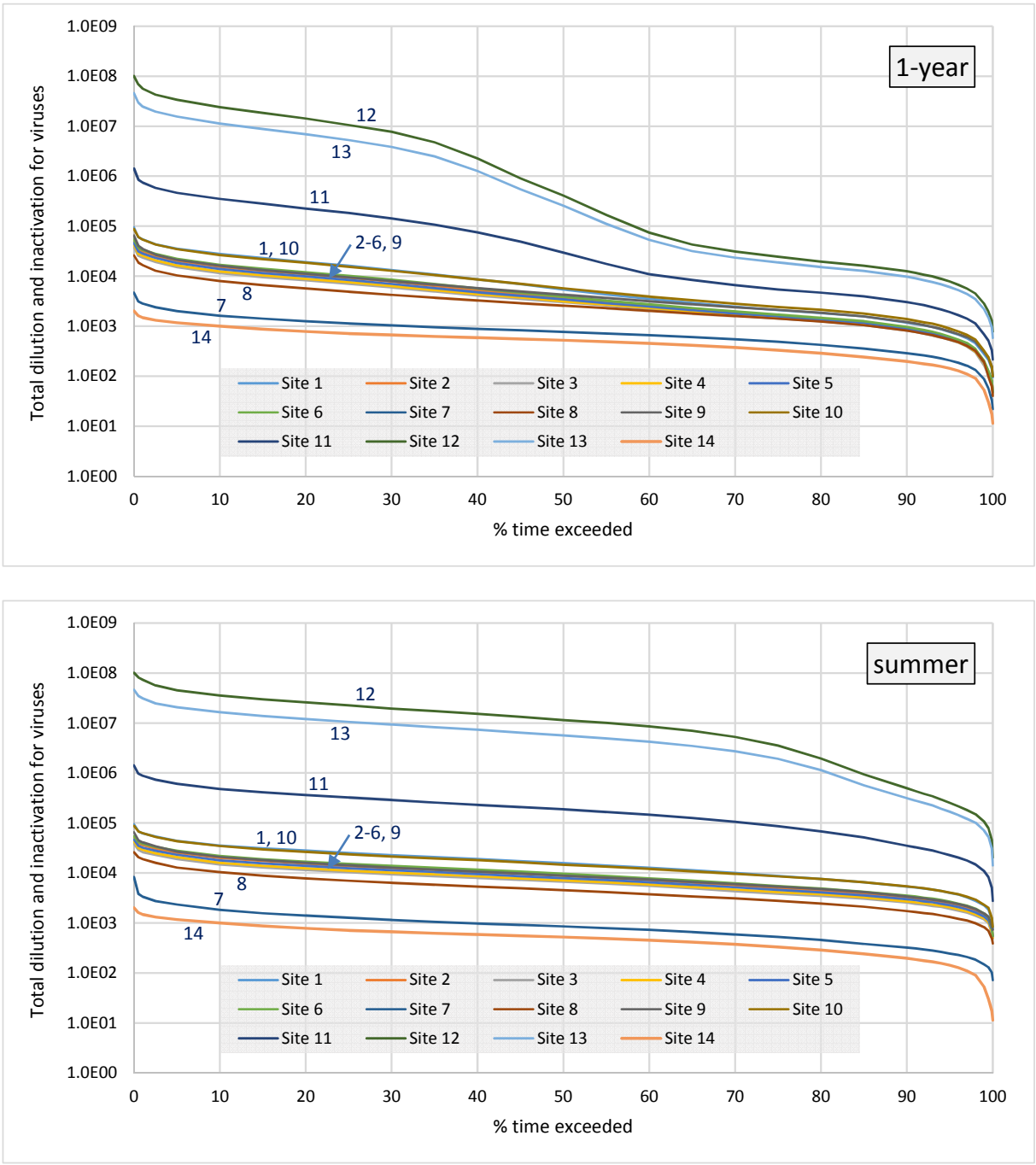

Figure 6-2: Cumulative distribution of total dilution plus inactivation (S_{tot}) for viruses at each of the specified sites of interest. (Top) for the entire 1-year simulation, (Bottom) for the summer bathing season (1 Nov - 31 Mar).

For the other sites besides site 14, median value of total dilution plus inactivation over the summer-bathing season ranges from 8.6×10^2 fold reduction at site 7–ExW (near the existing outfall south of Akaroa township) up to a 1.1×10^7 fold reduction at site 12–FFB in the upper Harbour (French Farm Bay) as listed in Table 6-2. The relatively lower dilutions that would be achieved at site 7–ExW arise from the eastern periphery of the dispersing ebb-tide plume that would sometimes brush this area as shown by the plume snapshots in Figure 5-3 and Figure 5-4. However the total dilution and inactivation at site 7–ExW from the proposed

outfall scheme will be substantially higher than the low dilutions presently being achieved in this area by the existing short outfall, 150 m to the north of site 7 (Figure 5-2).

Both upper-harbour sites 12–FFB and 13–TaB are predicted to show very large total dilutions plus inactivation (Figure 6-2), primarily due to the extensive microbial inactivation that will occur over the long travel times of over 8 days for the very dilute plume to reach these sites even in winter.

6.4 Final concentration-reduction CDFs

The final stage was to invert the total dilution and inactivation to a concentration-reduction factor to produce cumulative distribution functions (CDFs) of normalised concentrations (scaled to an effluent concentration of 1 virus/L) from the 1-year time series. These cumulative distribution functions are composed from sorting in ascending order around 35,000 values at 15-minute intervals from each of the 14 specified sites of interest.

The CDFs of normalised concentrations for each site are mirror images of the cumulative distributions shown for total dilution plus inactivation in Figure 6-2 and were delivered for input to the QMRA process (McBride, 2014).

7 Summary

This report summarises the dispersion modelling approach undertaken by NIWA for the proposed outfall in Akaroa Harbour and how the predicted dilutions and inactivation were determined for viruses at 14 pre-selected sites were derived for input to the QMRA process to assess the public-health risks from water-contact-recreation and raw shellfish consumption.

7.1 Results

Some key findings from the 1-year simulations:

- Initial dilution within the vicinity of the proposed outfall diffuser is one of the main contributors towards reducing virus concentrations at all of the coastal sites, followed closely by microbial inactivation, especially the more remote sites with long plume travel-times, while the smallest reduction is from subsequent dispersion (which incorporates slow overall flushing from the Harbour).
  - The median initial dilution is around 1480-fold, but decreases as the effluent discharge increases or the current velocity drops. Plume mixing with the receiving waters is much more efficient for lower discharges into faster current speeds.
  - Mostly, the far-field physical dilution factor is small at around 2–3 fold dilution, as it also includes the moderating effect of the harbour-wide flushing characteristics for the semi-enclosed Harbour (where a dynamic equilibrium is reached between the effluent discharge load (when modelled as a conservative tracer) and the volume exchanged each tide with the Canterbury Bight waters).
  - Average virus inactivation over the entire year ranged in a wide band from a 1.3-fold reduction at the middle Harbour site 14–MHb 160 m north of the proposed diffuser, 5-6 fold reduction covering sites 2-6 in French Bay, up to nearly 100-fold reduction for upper-harbour sites. These reductions due to microbial inactivation are directly reflected in the plume travel-time to each site, given the same hourly solar radiation (measured at the Akaroa EWS) was input to the inactivation algorithm for all sites.
- The approach of dis-aggregating the far-field physical mixing processes for a non-decaying substance and later factoring in microbial inactivation for viruses during post-processing is likely to be conservative by underestimating physical far-field dilutions at each site, particularly sites closer at hand to the outfall in the middle Harbour.
- The combined total dilution and inactivation achieved at all sites was slightly lower in winter (leaving aside the influence of wet-weather effluent flows) than in summer, even though the dry-weather effluent discharge rates are smaller (producing higher initial dilutions). This is due to the substantially lower microbial inactivation in winter.
- Based on median values, Site 14–MHb in the middle of the Harbour (160 m north of the proposed diffuser site) understandably produces the lowest total dilution plus inactivation of around 500-fold. For the other sites, total dilution plus inactivation over the summer-bathing season ranges from a median of 860-fold at site 7–ExW (near

the existing outfall south of Akaroa township) up to a 1.1×10^7 fold reduction at site 12–FFB in the upper Harbour (French Farm Bay). The lower dilutions that would be achieved at site 7–ExW (compared with the upper Harbour sites e.g., site 12), would arise from the eastern periphery of the dispersing ebb-tide plume brushing this area. However the total dilution and inactivation at site 7–ExW from the proposed outfall scheme will be substantially higher than that presently being achieved in this area by the existing short outfall 150 m to the north of site 7 (Figure 5-2) with the discharge from the present WWTP.

- Both upper-harbour sites 12–FFB and 13–TaB are predicted to yield very large total dilutions plus inactivation, primarily due to the extensive microbial inactivation of nearly 100-fold that will occur over the long travel times of over 8 days for the very dilute plume to reach these sites.

7.2 Deliverables

The final stage was to invert the total dilution plus inactivation to a concentration-reduction factor to produce cumulative distribution functions (CDFs) of normalised concentrations (scaled to an effluent concentration of 1 virus/L) from the 1-year time series. The more than 35,000 15-minute values at each of the 14 sites of interest were sorted into ascending order and percentile values calculated to define the cumulative distribution functions.

For the QMRA analysis, Graham McBride (NIWA) was supplied these cumulative distribution functions for each of the selected sites, which were normalised to an effluent concentration of 1 virus/L and only require multiplying by a final-effluent virus concentration in viral units per litre, to get concentrations at each site.

8 Acknowledgements

The authors wish to thank the following people or agencies who provided services or data:

- Warren Thompson, Chris Woods and Lindsay Hawke from the Christchurch NIWA office who coordinated and carried out the field programme for Akaroa Harbour including the ADP and tide-gauge deployments.
- Instrument Services (NIWA) for supplying and calibrating the tide gauge.
- Christchurch City Council for supplying wind data from the weather station at the proposed WWTP site.
- University of Canterbury (Dr Deidre Hart) and Environment Canterbury for providing bathymetric data for the upper Harbour.
- Land Information NZ for supply of bathymetric data for the entire Harbour from the LINZ Data Centre portal.
- Dr Derek Goring (Mulgor Consulting Ltd) for supplying sea-level data from the 2008 deployments of gauges for a CCC project.
- Harbourmaster (Jim Dilley) for processing the ADP deployment notices to mariners and advising on the best location to deploy.
- Dr Mark Pritchard (NIWA) for providing Delft2d modelling advice.
- Graham McBride for his advice and encouragement during the study.
- Scott Stephens and Andrew Swales for thorough peer reviews.
- Bridget O'Brien, Graeme Jenner, Greg Offer and Reuben Bouman (CH2M Beca) and Ian Goss (OCEL Consulting) who provided various datasets on the WWTP effluent discharges and proposed outfall.

9 Glossary of abbreviations and terms

ADF	Average Daily Flow for the effluent discharge over a long period.
ADP	Acoustic Doppler Profiler current-meter that measures current velocity in different depth layers in the water column.
concentration-reduction factor	Essentially, the concentration at each site for a virus effluent concentration of 1 virus/L. This normalised factor can then be multiplied by the virus concentration in the effluent to derive predicted concentrations at each coastal site. The inverse is the total dilution achievable at each site including virus inactivation.
diffuser	Regularly spaced outlets (ports) at the end of an outfall pipe for releasing the treated effluent at high velocity.
dispersion	Physical process of mixing and dilution of a discharge with a receiving water-body in the far-field phase through advection (plume stretching from spatially-varying currents and wind effects) and diffusion (turbulent eddy mixing and lateral and vertical spreading).
effluent	Treated wastewater delivered from the WWTP to the outfall to be discharged through the diffuser.
enteric viruses	An important, but diverse, group of viruses found in the intestinal tract of humans and animals e.g., adenoviruses, noroviruses (Norwalk-like viruses), rotaviruses, enteroviruses.
EWS	Environmental Weather Station.
far-field phase	Occurs beyond the zone of initial dilution, where mixing and dilution processes that disperse the plume (at length scales of 100's of metres to a few kilometres) are dominated by environmental conditions (e.g., tides, winds). In a semi-enclosed harbour like Akaroa, basin-wide mixing and flushing process at longer spatial and time scales (weeks to months) will also affect the overall far-field physical dilution that can be achieved and is intricately connected with the time-rate of decay for discharged substances or inactivation of viruses.
influent	Raw sewage from the sewerage network that is received at the WWTP.
initial dilution	Physical dilution processes that occurs in the near-field phase in the immediate vicinity of the diffuser (near-field) until the plume has reached the surface or a neutrally-buoyant state.
microbial inactivation	Reduction in viable microbial (bacteria or virus) numbers in receiving waters due primarily to cell impairment or death associated with solar radiation (UV and short-visible wavelengths) and to a lesser extent temperature, salinity and grazing by micro-fauna.
MSL	Present-day mean sea level (usually over a period of a year or more).

near-field phase	Where the buoyancy (from the freshwater effluent), momentum of the jets from the diffuser and the current speed across the diffuser govern the mixing processes within close proximity to the outfall diffuser. For the proposed Akaroa outfall, the near-field extends only 50-100 m, with most of the mixing complete by around 50 m from the diffuser.
QMRA	Quantitative Microbial Risk Assessment.
solar radiation	Irradiance (energy) from the Sun in mega-Joules per square metre (MJ/m^2) received at the Earth's surface accumulated over a defined time interval e.g., 1 hour typically – in this case called “hourly solar radiation”.
subsequent dilution	Physical dilution that occurs following the initial dilution phase when environmental conditions (winds, tides, currents) dictate the dispersion of the plume rather than the initial discharge characteristics. Also includes the basin-wide mixing and flushing characteristics.
WWTP	Wastewater Treatment Plant.

10 References

Bell, R.G., Munro, D., Powell, P. (1992) Modelling microbial concentrations from multiple outfalls using time-varying inputs and decay rates. *Water Science and Technology,* 25(9): 181–188.

Deltares (2011) Delft-3D-Flow: Simulation of multi-dimensional hydrodynamic flows and transport phenomena, including sediments. *User Manual Version 3.15*: 672.

Doneker, R.L., Jirka, G.H. (2012) CORMIX User Manual*. A hydrodynamic mixing zone model and decision support system for pollutant discharges into surface waters.* U.S. Environmental Protection Agency. Washington D.C.

Goring, D.G. (2008) Datums in Akaroa Harbour from tide gauge analysis*. Report to Christchurch City Council*: 10.

Greig, M.J., Ridgway, N.M., Shakespeare, B.S. (1988) Sea surface temperature variations at coastal sites around New Zealand. *New Zealand Journal of Marine and Freshwater Research,* 22: 391–400.

Hart, D., Todd, D.J., Nation, T.E., McWilliams, Z.A. (2009) Upper Akaroa Harbour seabed bathymetry and soft sediments: A baseline mapping study*. University of Canterbury Coastal Research Report 1*, prepared for Environment Canterbury as ECan Report 09/44: 35 + Appendices.

Heath, R.A. (1976) Broad classification of New Zealand inlets with emphasis on residence times. *New Zealand Journal of Marine and Freshwater Research,*10: 429–444.

Hicks, D.M., Marra J.J. (1988). Coastal processes and conditions in French Bay, Akaroa Harbour. *Unpublished report prepared for Akaroa Marina Co*.: 48 (cited in Hart et al. 2009).

Heuff, D.N., Spigel, R.H., Ross, A.H. (2005) Evidence of a significant wind-driven circulation in Akaroa Harbour. Part 1: Data obtained during the September–November, 1998 field survey. *NZ Journal of Marine & Freshwater Research,* 39: 1097–1109.

Jerlov, N.G. (1976) Marine optics. *Elsevier Oceanographic Series* No. 14, Elsevier, The Netherlands.

Jirka, G.H., Doneker, R.L., Barnwell, T.O. (1991) CORMIX: A comprehensive expert system for mixing zone analysis of aqueous pollutant discharges. *Water Science and Technology,* 24(6): 267–274.

LINZ (2008) Land Information New Zealand. *Akaroa Harbour Hydrographic Surveys: 1:20,000 Standard Sheet AK-STD-01 and 1:10,000 French BayAKFB-STD-01, and Report of Survey.* Prepared by Discovery Marine Ltd, Mount Maunganui, New Zealand. 1 map sheet: 16 report.

LINZ (2009) Akaroa Harbour. *Hydrographic Chart NZ6324*. Published by Land Information NZ.

LINZ (2013) *New Zealand nautical almanac, 2013/14 Edition*, Publication NZ 204.

McBride, G. (2014) Water-related Health Risks Analysis for the proposed Akaroa wastewater scheme. *NIWA Client Report* HAM2014-030, prepared for CH2M Beca Ltd.

Pawlowicz, R. (2002) Classical tidal harmonic analysis including error estimates in MATLAB using T-tide. *Computers & Geosciences, 2*8: 929–937.

Walters, R.A., Goring, D.G., Bell, R.G. (2001) Ocean tides around New Zealand. *NZ Journal of Marine & Freshwater Research,* 35(4): 567–579.

Williams, B.L. (Ed.) (1985) Ocean Outfall Handbook. *Water and Soil Miscellaneous Publication* 76, National Water and Soil Conservation Authority, Ministry of Works & Development, Wellington.

Wood, I.R., Bell, R.G., Wilkinson, D.L. (1993) *Ocean Disposal of Wastewater*, Advanced Series on Ocean Engineering – Vol. 8, World Scientific Publishing Co., Singapore: 425.

11 Appendix 1: Virus inactivation in wastewater plumes

Compiled by G. McBride (NIWA)

In developing a water quality model for pathogenic viruses we need to incorporate UV-inactivation processes in a rigorous manner—incorporating dark versus light conditions (including shading), seasonality, vertical UV attenuation, and cloudiness.

There are a number of inactivation studies for bacteria in water (e.g., Auer & Niehaus, 1993, Noble et al. 2004, Hipsey et al. 2008), but many fewer for viruses. In many ways the best we have are the New Zealand studies by Sinton and colleagues which considered sunlight inactivation of phages and bacteria in river water and seawater mixed with sewage. Sinton et al. (1999, 2002) used Lyttelton Harbour seawater, into which they placed some sewage. So to the extent that predators were already in that seawater, some predation by micro-fauna would have occurred, which is presumably reflected in the night-time ("dark") inactivation. In these studies Sinton et al. (1999, 2002) studied faecal coliforms, *E. coli*, enterococci, somatic coliphages and F-RNA phages. Phages can be seen as surrogates for pathogenic viruses.

Accounting for time-varying inactivation in aquatic modelling has most often used a “time-based” approach using a time-varying inactivation coefficient assuming first-order kinetics for inactivation related to incoming irradiance and for “dark” inactivation (e.g., Noble et al. 2004). That is expressed by the single-parameter model

$$\frac{\mathrm{d}C}{\mathrm{d}t} = -k(t)C: \quad k = k_d + k_I(t) \tag{1}$$

where C is microbe concentration, t is elapsed time (hours) and k (h^{-1}) is the time-varying inactivation coefficient comprised of a constant “dark” component (k_d) and a time-varying “light” component (k_I). The dark processes especially include grazing by larger microbes (which also occurs during the day) and the light processes particularly refer to solar irradiance.

However, Sinton et al. (1999, 2002) have noted that it may be more appropriate (and less complex) to replace the varying time-based inactivation coefficient with a constant coefficient (k_s) multiplied by time-varying irradiance. In that way the inactivation rate can be indexed to actual environmental conditions. The first-order model is then

$$\frac{\mathrm{d}C}{\mathrm{d}t} = -k(t)C: \quad k = k_d + k_s G(t) \tag{2}$$

where k_s (m^2 MJ^{-1}) is the sunlight inactivation coefficient (corrected for dark inactivation) and $G(t)$ is time varying irradiance (MJ m^{-2} h^{-1}). This formulation provides for a hugely less complicated algorithm, so it is highly advantageous to have records of nearby insolation available.

Two caveats must now be made.

First, as noted by Craggs et al. (2004):

> "… only a minor portion of the total solar irradiance that penetrates the water is responsible for disinfection. Davies-Colley et al. (1997, 1999) found that solar UV wavelengths in the range from 290 to 400 nm and centred around 340 nm were mainly responsible for solar disinfection…. However, transmission of the biologically active part of the solar UV spectrum is difficult to measure, and is only weakly related to (and much smaller than) the penetration of visible light into … water, so we have chosen to neglect this refinement for now."

They also noted that a proportion (~10%) of this biologically active UV radiation is reflected at the pond surface, and the remainder is attenuated down the water column. These features are rather more easily accounted for.

Second, Sinton et al. (1999, 2002) have observed that the progress of inactivation (with insolation) often exhibits a "shoulder", in which the inactivation onset is resisted for some time (possibly by microbial self-repair mechanisms). This effect was particularly pronounced for their bacteria experiments in which raw sewage was mixed with river water—it was less so for waste stabilisation pond effluent mixed with river water. No shoulder effect was observed for phages so this caveat can be ignored, and a simple first-order inactivation model is appropriate.

So we use these values:

Table A-1 Phage Inactivation coefficients.

Parameter	Summer	Winter
k_d (h^{-1})	0.044	0.015
k_s ($m^2\ MJ^{-1}$)	0.07	0.05

Notes: k_d = first-order *dark* inactivation coefficient (base e), from Table 2 in Sinton et al. (1999); k_s = first-order insolation-based daytime inactivation coefficient Table 3 in Sinton et al. (1999).

Calculation procedure

We first calculate k_s then calculate the inactivation over a given time interval.

Seasonality in k_s is handled by making appropriate interpolations between summer and winter conditions. We use a simple sigmoidal function[9] with the general formula

$$k_s = \begin{cases} k_{s,\text{winter}} & D = 0 \\ k_{s,\text{winter}} + \dfrac{k_{s,\text{summer}} - k_{s,\text{winter}}}{1 + e^{6-12D/182}} & 1 \le D \le 182 \\ k_{s,\text{summer}} & D = 183 \end{cases} \qquad (3)$$

where D is days before (or until) winter solstice. A similar equation is used for $k_{d,}$.

Cloudiness is handled by multiplying k_s by the ratio of daily insolation to maximum possible insolation for that day.[10]

[9] These functions have the general form $f(x) = 1/(1 + e^{-x})$.
[10] Most of the experiments by Sinton et al. (1999) were for clear skies.

Vertical UV attenuation is handled via the standard factor

$$f(\zeta) = \frac{1 - e^{-\zeta}}{\zeta} \tag{4}$$

where $\zeta = K_{att}d$ is optical depth, in which K_{att} is the vertical UV attenuation coefficient (~1 m^{-1}) and d (m) is the appropriate depth (e.g., of a diluted sewage plume). The k_s term is multiplied by this factor.

Calculating inactivation over a time period Δt

Simple integration of equation (2) from time t_0 to time t gives the required reduction ratio as

$$\delta C = \frac{C(t)}{C(t_0)} = \mathrm{e}^{-[k_d + \mathrm{f}(\zeta)\phi k_s \Delta S(t)]\Delta t} \tag{5}$$

where ϕ is the fraction of incident UV that is not reflected from the water surface and

$$\Delta S(t) = \int_{\xi=t_0}^{\xi=t} G(\xi)\mathrm{d}\xi \tag{6}$$

is insolation over the period $\Delta t = t - t_0$ (MJ m^{-2} H^{-1}).

References

Auer, M.T., Niehaus, S.L. (1993) Modeling fecal coliform bacteria - I. Field and laboratory determination of loss kinetics. *Water Research,* 27: 693–701.

Craggs, R.J., Zwart, A., Nagels, J.W., Davies-Colley, R.J. (2004) Modelling sunlight disinfection in a high rate pond. *Ecological Engineering,* 796: 1–10.

Davies-Colley, R.J., Donnison, A.M., Speed, D.J. (1997) Sunlight wavelengths inactivating faecal indicator microorganisms in waste stabilisation ponds. *Water Science and Technology,* 35: 219–225.

Davies-Colley, R.J., Donnison, A.M., Speed, D.J., Ross, C.M., Nagels, J.W. (1999) Inactivation of faecal indicator micro-organisms in waste stabilisation ponds: interactions of environmental factors with sunlight. *Water Research,* 33: 1220–1230.

Hipsey, M.R., Antenucci, J.P., Brookes, J.D. (2008) A generic, process-based model of microbial pollution in aquatic systems. *Water Resources Research,* 44: 1–26.

Noble, R.T., Lee, I.M., Schiff, K. (2004) Inactivation of indicator bacteria from various sources of fecal contamination in seawater and freshwater. *Journal of Applied Microbiology,* 96: 464–472.

Sinton, L.W.F., Finlay, R.K., Lynch, P.A. (1999) Sunlight inactivation of fecal bacteriophages and bacteria in sewage-polluted seawater. *Applied and Environmental Microbiology,* 65: 3605–3613.

Sinton, L.W., Hall, C.H., Lynch, P.A., Davies-Colley, R.J. (2002) Sunlight inactivation of fecal indicator bacteria and bacteriophages from waste stabilization pond effluent in fresh and saline waters. *Applied and Environmental Microbiology,* 68(3): 1122–1131.

12 Appendix 2: Measures of model skill and accuracy

Bias is a measure of the overall offset between the model predictions and the observations. The most common measure of bias uses the mean of the differences, although there are circumstances where using the median is appropriate. Bias is sometimes referred to as reliability. In this definition a "reliable" model does not consistently over-predict or under-predict, but is not necessarily accurate (Sutherland et al. 2004).

$$Bias = \frac{1}{n}\sum_{i=1}^{n}\left(y_i - x_i\right) \quad (1)$$

Where: x_i is the modelled, y_i the measured value, and n the number of values being compared.

Accuracy is a measure of difference between a prediction and the corresponding observations. The average accuracy can be represented in a dimensional or a non-dimensional (relative accuracy) manner.

The **root mean square error (RMSE)** has been used as a statistical measure of the dimensional model accuracy.

$$RMSE = \sqrt{\frac{1}{n}\sum_{i=1}^{n}\left(y_i - x_i\right)^2} \quad (2)$$

Where: x_i is the prediction and y_i the true value and n the number of values being compared.

Model skill is a measure **(*SKILL*)** where values span 1 (high) to 0 (poor) skill decreases towards zero as described by Warner et al. (2005) and Haidvogel et al. (2008). *SKILL* is defined as:

$$SKILL = 1 - [|X_m - X_o|^2] / \left[\sum_{i=1}^{N}(|X_{mi} - \overline{X_o}| + |X_{oi} - \overline{X_o}|)^2\right], \quad (3)$$

where X is a variable and $\bar{X}$ is a time average of the variable. Subscript m and o are for modelled and observed values respectively.

Cross correlation function (R_{xy}) is a statistical method of quantifying the similarity between two waveforms as a function of a time-lag between two time series data sets. For example, the timing of an observed and modelled tidal curve. This is computed from the cross-covariance function:

$$C_{xy}(\tau) \equiv E\left[\left\{y(t) - \mu_y\right\}\left\{x(t+\tau) - \mu_x\right\}\right] \quad (4)$$

Where: C_{xy} is the cross-covariance function, E is the expected value, $x(t)$ and $y(t)$ are discrete variables at time t, μ_y and u_x are means of the time series, and τ is the time lag.

The cross correlation function (R_{xy}) is a non-dimensional summary of this analysis which ranges from 0 to 1, where 1 infers a strong phase agreement between the two signals.

$$R_{xy} \equiv \frac{C_{xy}(\tau)}{\sigma_x \sigma_y} \quad (5)$$

Where: σ_x, σ_y are the standard deviations of each time series.

References

Haidvogel, D.B., Arango, H., Budgell, W.P., Cornuelle, B.D., Curchitser, E., Lorenzo, E. Di., Fennel, K., Geyer, W.R., Hermann, A.J., Lanerolle, L., Levin, J., McWilliams, J.C., Miller, A.J., Moore, A.M., Powell, T.M., Shchepetkin, A.F., Sherwood, C.R., Signell, R.P., Warner, J.C., Wilkin, J. (2008) Ocean forecasting in terrain-following coordinates: Formulation and skill assessment of the Regional Ocean Modeling System. *Journal of Computational Physics,* 227: 3595–3624.

Sutherland, J.; Peet, A.H.; Soulsby, R.L. (2004). Evaluating the performance of morphological models. *Coastal Engineering 51(8–9)*: 917–939.

Warner, J.C., Geyer, W.R., Lerczak, J.A. (2005) Numerical modeling of an estuary: A comprehensive skill assessment. *Journal of Geophysical Research-C,* 110, C05001, doi: 10.1029/2004JC002691.